DISSERTATIONES
CHIMICAE
UNIVERSITATIS
TARTUENSIS
160

KRISTJAN HAAV

Quantitative relative equilibrium constant measurements in supramolecular chemistry

DISSERTATIONES CHIMICAE UNIVERSITATIS TARTUENSIS
160

DISSERTATIONES CHIMICAE UNIVERSITATIS TARTUENSIS
160

KRISTJAN HAAV

Quantitative relative equilibrium constant measurements in supramolecular chemistry

UNIVERSITY OF TARTU
Press

Institute of Chemistry, Faculty of Science and Technology, University of Tartu, Estonia

Dissertation is accepted for commencement of the degree of Doctor of Philosophy in Chemistry on June 14th, 2017 by Council of Institute of Chemistry, University of Tartu

Supervisors: Prof Ivo Leito, PhD
Institute of Chemistry, University of Tartu, Estonia

Opponent: Prof. emer. Jean-Francois Gal
Institut de Chemie de Nice, France

Commencement: August 16th, 2017, 10.00
Ravila Street 14a, Tartu (Chemicum), auditorium 1021

This work has been partially supported by Graduate School of Functional materials and technologies receiving funding from the European Reginal Development Fund in University of Tartu, Estonia

ISSN 1406-0299
ISBN 978-9949-77-480-7 (print)
ISBN 978-9949-77-481-4 (pdf)

University of Tartu Press
www.tyk.ee

CONTENTS

LIST OF ORIGINAL PUBLICATIONS

I K. Haav, J. Saame, A. Kütt, I. Leito, Eur. J. Org. Chem. 2012, 2167–2172.

II K. Haav, S. A. Kadam, L. Toom, P. A. Gale, N. Busschaert, M. Wenzel, J. Hiscock, I. Kirby, T. Haljasorg, M. Lõkov, I. Leito, J. Org. Chem. 2013, 78, 7796 –7808.

III S. A. Kadam, K. Haav, L. Toom, T. Haljasorg, I. Leito, J. Org. Chem. 2014, 79, 2501 –2513.

IV S. A. Kadam, K. Martin, K. Haav, L. Toom, C. Mayeux, A. Pung, P. A. Gale, J. R. Hiscock, S. J. Brooks, I. L. Kirby, N. Busschaert, I. Leito, Chem. Eur. J. 2015, *21*, 5145–5160.

V S. Tshepelevitsh, A. Trummal, K. Haav, K. Martin, I. Leito, J. Phys. Chem. A 2017, *121*, 357–369.

VI S. A. Kadam, K. Haav, L. Toom, A. Pung, C. Mayeux, I. Leito, Eur. J. Org. Chem. 2017, 1396–1406.

Author's contribution

Paper I. Performed all pK_a measurements and data analysis. Main person responsible for writing the manuscript.

Paper II. Planned, developed and performed all the binding affinity measurements. Main person responsible for writing the manuscript.

Paper III. Helped to plan and develop NMR measurement methods. Planned and performed the UV-vis spectrophotometry experiments. One of the main person responsible for writing the manuscript.

Paper IV. Planned binding affinity experiments and supervised part of the experiments. One of the main person responsible for writing the manuscript.

Paper V. Responsible for planning the logK_{ass} experiments and performing part of them. Participated in writing experimental section manuscript and in revision.

Paper VI. Responsible for planning, supervising the binding experiments and data analysis. Also, responsible for planning and writing the manuscript.

ABBREVATIONS

a	Activity
α	Empirical parameter for solvent HBD acidity
A^{λ}	Absorbance at given wavelength
AN	Acceptor number
β	Empirical parameter for solvent HBA basicity
$CHCl_3$	Chloroform
DN	Donor number
DMSO	Dimethyl sulfoxide
EPA	Electron-pair acceptor
EPD	Electron-pair donor
ε_r	Relative permittivity
Gly^{2-}	Glyphosate dianion
HB	Hydrogen bond
HBA	Hydrogen bond acceptor
K_{ass}	Binding/association constant
$\log K_{ass}$	Logarithm of binding/association constant
$\log P_{octanol\text{-}water}$	Logarithm of octanol-water partition coefficient
MeCN	Acetonitrile
pK_a	Negative logarithm of acid dissociation constant
PCA	Principal component analysis
TBA	Tetrabutylammonium

1. INTRODUCTION

Synthetic anion receptors in supramolecular chemistry are of growing interest for analytical chemists for their potential use in chemical analysis. Classical instrumental methods of anion determination are often expensive, time consuming and complex to use. Introduction of supramolecular sensing elements – synthetic anion receptors – can in principle be used for the development of cheap and robust methods. By implementing them into analytical devices – sensors – they can become useful sensing elements to detect analytes in complex samples. One of the first steps in this process is to test their sensitivity and selectivity towards target analytes. Association (binding) constant K_{ass} is the key characteristic for evaluating both sensitivity and selectivity: K_{ass} is a direct quantitative measure of sensitivity and ratios of K_{ass} values (differences of $\log K_{ass}$ values) towards the same anion give information about selectivity. Accurate quantification of equilibrium constants is a challenging task. In terms of anion binding by synthetic receptors, anion activity, one of the inputs in binding constant calculation, can be affected by several solvent effects, such as homoconjugation and ionpairing, making its accurate determination difficult. The same difficulties are observed in measurements of other equilibrium constants, especially in nonaqueous solutions.

The goal of this thesis was the development of relative equilibrium constant measurement methods – i.e. methods that measure equilibrium constant ratios (or differences of their logarithms) rather than the absolute equilibrium constants. The rationale behind this is that a number of uncertainty sources are reduced or eliminated by this. As the first stage, UV-vis spectrophotometry is applied to measure the relative basicity of a set of phosphanes and diphosphanes and binding of synthetic receptors towards target anion acetate. Further development of the relative binding affinity measurement is achieved by implementing the method on NMR.

The proposed methods are used to demonstrate how to overcome limitations of direct K_{ass} measurements. Binding constant measurement method development is carried out in parallel with carboxylate binding studies. Carboxylates are key species in different areas, including industry, pharmacy, biology and medicine. Carboxylates ranging from lipophilic to hydrophilic were included to quantify their binding and further improve the understanding of relationships between structure, binding sensitivity and selectivity. Also, binding of a widely used pesticide – glyphosate is characterized by its binding properties in different DMSO:H_2O mixtures. Glyphosate determination via solid phase extraction (SPE) in conjunction with LC/ESI-MS or GC/MS is difficult because of its high hydrophilicity and therefore poor extraction efficiency from samples, as well as unsuitability for both LC and GC as separation methods. Synthetic receptors could potentially improve glyphosate extraction from aqueous samples or used as sensing elements in sensors.

2. LITERATURE OVERVIEW

2.1. Supramolecular chemistry

2.1.1. Background

Supramolecular chemistry is a field of chemistry that goes beyond individual molecules and focuses on non-covalently bound molecular assemblies. By concept it has been given several definitions. Perhaps the most familiar is "chemistry beyond the molecule".[1] Also, it is known as "chemistry of molecular assemblies and of intermolecular bond" and "chemistry of the non-covalent bond".[1–3] Interaction of molecular species by non-covalent bonds is a key characteristic for making clear distinction between supramolecular assemblies and "conventional" molecules where bonds have covalent nature and are in most cases not reversible. The pioneers of supramolecular chemistry J.-M. Lehn[4], D. J. Cram[5] and C. J. Pedersen[6] were awarded with a joint Nobel prize in chemistry in 1987 for their contributing works in field of supramolecular chemistry. Their work involved design and synthesis of crown ethers and cryptands and complexation studies of alkali and alkaline earth metal ions.

In binding process we define one molecule as a host which binds another species, defined as a guest.[3] Usually molecule that is larger in size is referred to as host (receptor) and smaller species as guest (in some cases also called substrate). Hosts can be large molecules or formed aggregates such as enzymes in biological systems or synthetic receptors. Guests can be monoatomic cations, inorganic anions, ion pairs or molecules. Sometimes both host and guest can be similar in size. For better distinguishing host is viewed as species having binding sites such as Lewis basic donor atoms or hydrogen bond donors. Guest has Lewis acidic metal cation or hydrogen bond acceptor binding sites.[3]

More specific and characteristic interactions have led to molecular devices,[7] molecular recognition,[8,9] self-assembly[10,11] and self-organization.[12] The term molecular species does not always hold as also inorganic metal cations or anions can participate in formation of complex by bonds of non-covalent nature.

In host-guest chemistry complementary binding of the two species is important. Use of directional bonds (donor-acceptor, hydrogen bonding) can improve selectivity of a given interaction. Specific binding can be achieved also by lock and key analogy[1] where binding site of host is shaped accordingly to the guest. Since molecular recognition is based on non-covalent bonds their strength is highly dependent on external parameters like solvent composition, polarity and even temperature.[13]

2.1.2. Anion coordination

Anion coordination chemistry is a diverse field as anions come in different shapes, sizes, charge and charge localization.[14–16] Anionic species are key components in biological systems, medicine and industry. Simple inorganic anions

such as chloride, carbonate, nitrate and sulfate are present in the environment. Many pharmaceuticals are in the form of anions in aqueous solution. And monitoring their residues in environment is an important task. Moreover, majority of enzyme substrates and cofactors are present as anions.[17]

Some of the first reported anion binding receptors were based on protonated polyamines.[18–21] Additionally guanidinium based receptors have found use.[22–24] Using protonated amines or guanidines takes similarities from biological systems as these structural elements are also present in amino acids lysine and arginine, which are building blocks of proteins. In these cases binding interactions are mostly driven by charge-charge attraction that is accompanied by hydrogen bonding. Charged receptors tend to have the advantage as charge-charge interaction is often stronger than hydrogen bonding. Neutral hydrogen bond donor based receptors emerged by the use of pyrrole[25] and amide[22] motifs.

Design of synthetic hosts that are complementary to target anion is a big challenge. In addition to large variety, anions have some characteristic properties that can complicate receptor design. Anions may have certain pH range where they have negative charge. Designed host must also function then in the given pH range. This puts some limitations for charged receptors that might become neutral at certain pH conditions. As said there is a large variety in shapes and geometries. Even in case of inorganic anions, the structures vary from spherical (halides), linear (SCN^-, N_3^-), planar (NO_3^-), tetrahedral (PO_4^{3-}, SO_4^{2-}) to octahedral (PF_6^-). Biologically important anions such as phosphorylated molecules (AMP, ADP, ATP) are even more complex by structure.[26] Because coordinative saturation of anions binding can mostly happen with weaker forces like hydrogen bonds and van der Waals interactions.

2.1.3. Supramolecular analytical chemistry

Supramolecular analytical chemistry is chemistry where host-guest chemistry and molecular recognition have been applied in analytical applications.[27] Aim is to mimic the behavior of natural receptors to selectively bind specific species. In the context of analytical chemistry this would be recognition of analyte molecules in samples containing also a complex mixture of matrix components. Introduction of receptors that can recognize analytes at low concentration levels can be in turn used to introduce new analytical methods or improve sample preparation methods.[28–30] Scheme 1 presents a potential construction of a supramolecular sensing element. Based on signal recognition mechanism and operating principle the receptors can be divided into different classes. Optical receptors are the ones where analyte binding to the receptor causes changes in optical properties of the receptor. The respective change can be quantified by measuring absorbance, luminescence, and reflectance. In electrochemical receptors analyte binding produces a change in electrochemical properties (current, potential in ion selective electrode). Electrical receptors experience change during receptor-analyte interaction in electrical properties (conductivity, permittivity).

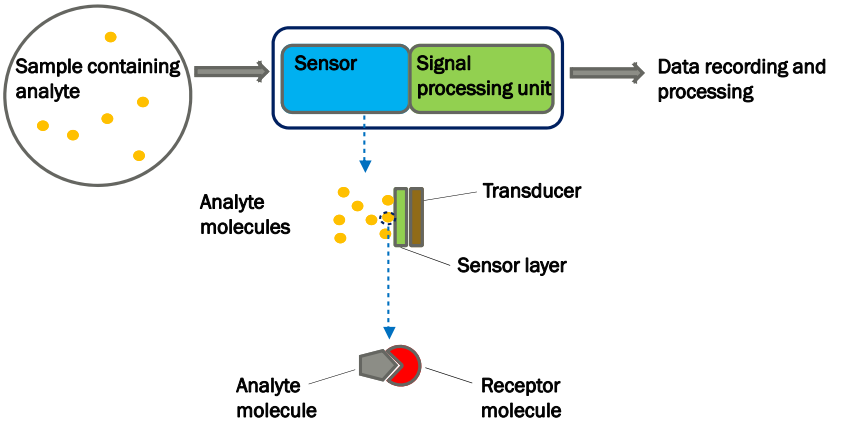

Scheme 1. Structure of supramolecular sensing element.

Receptor design has followed mainly two pathways. Firstly, the quest for designing a receptor specific for a single analyte. Numerous work have been published pursuing the challenges in synthesizing such compounds.[15,31–36] Achieving specific binding of anions by synthetic receptors is tremendously difficult task. The second approach is to use differential sensing.[37] In that case specificity is not a must and pattern of selective binding is created by employing a range of receptors. This sensing works in a similar manner to how we feel taste and sense smell a pattern recognition is created by an array of non-specific receptors that are cross-reactive towards a range of analytes.[30] Whether a single analyte or multiple analytes are bound, each receptor binds analytes differently and thus a response pattern is created by the receptors.

2.2. Supramolecular interactions

For anion sensing it is important that binding is sensitive, selective and reversible. Non-covalent interactions are the best choice to meet these considerations. A wide range of interactions fall under the category of non-covalent bonding. Formation of supramolecular complexes (supermolecules) is often based on interplay of several weak interactions. Although individually weak, they can in cooperation achieve very good sensitivity. Use of directional interactions enables to tuning selectivity.

2.2.1. Hydrogen bonding

Hydrogen bonding (HB) is an interaction of high interest to supramolecular chemistry.[38] It is both directional and has considerable bond strength, usually in the range of 3–46 kJ mol^{-1} in various solvents.[39] Directionality of bond offers better possibility to adjust selectivity. The strength of HB is set by the properties of HBD and HBA, partial charges of donor and acceptor and bond angle. By

definition hydrogen bond is formed when a hydrogen atom, covalently bound to an electronegative atom, forms a second bond to another atom with negative partial charge.[40,41] Equation (1) describes formation of hydrogen bond between R-X-H and :Y-R'. X and Y are atoms with higher electronegativity than hydrogen.

$$R-X-H+:Y-R' \rightleftharpoons R-X-H\cdots Y-R' \quad (1)$$

In the case of receptor-anion interaction the HBA is anionic: $^{-}$Y-R'. Hydrogen bonds can be either intermolecular or intramolecular. The nature of interaction in HBs is complex. It shares similarities both to covalent and ionic bonds.[40] Strong hydrogen bonds have larger covalent component, often called quasi-covalent bonds[42] and bond energy 60–160 kJ mol^{-1}. Moderate (16–60 kJ mol^{-1}) and weak (<16 kJ mol^{-1}) hydrogen bonds are more similar to electrostatic interaction.[40] For strong hydrogen bonds, the bond angle is in quite a narrow range of 175–180º, for moderate (130–180º) and weak (90–180º) hydrogen bonds the angles are wider and more flexible.

The most common hydrogen bond donor sites are R-OH, R-CO-NH- and R-N^{+}-H. Hydrogen bond acceptor sites can be anions, carbonyl bond (amides, ureas, esters), oxides (sulfoxides, phosphine oxides), alcohols, *etc*.[43]

Hydrogen bonding is one of the main interactions in supramolecular chemistry and at the same time it is the first step in an acid-base reaction.[13] If the HBD is sufficiently strong Brønsted acid and the HBA is strong Brønsted base then proton transfer might occur, often leading to formation of hydrogen bond between the formed anion and cation.

2.2.2. Ion-ion bonding

Ionic bonding is one of the strongest of non-covalent interactions and has bond energies close to those of covalent bonding (100–350 kJ mol^{-1}).[44] In solution it is responsible for ion pairing and salt bridge phenomena. Interaction strength is largely dependent on charge size and distance between charges. In case of molecular species, also, charge localization over the molecule affects binding strength – the more localized the charge the stronger the binding. Ion-ion interaction is non-directional and binding takes place purely via electrostatics. Thus, intrinsically this interaction has low selectivity of binding. However, selectivity can be achieved by designing host with complementary binding pocket. While studying anion binding to receptors, anions are usually in the form of salts. Because of that ion pairing of anion with its positively charged counter ion can also influence the process. In anion-receptor binding studies Bu_4N^{+} salts are commonly used, in which the ion pairing effect is considerably reduced. Still it has been found that in nonpolar solvents only small part of Bu_4N^{+} salts are dissociated.[45]

2.2.3. Ion-dipole interaction

Ion-dipole interaction takes place between electrically neutral molecule that possesses a permanent dipole moment and an ion.[13] The dipole orients itself so that the opposite partial charge will be facing the ion, causing attractive interaction. Even formation of hydrogen bond between negatively charged anion (carboxylic group in acetate) and neutral molecule with positive partial charge (e.g. N-H moiety in urea) can also be partially viewed as a form of ion-dipole. The strength of ion-dipole interaction can vary greatly (50–200 kJ mol^{-1}).[44] It depends on permanent charge of the ion, polarizability of dipole and on the angle at with the ion and dipole interact.

2.2.4. Aromatic interaction

Aromatic interactions can have significant effect on supermolecule stability (e.g., stacking of bihelix of DNA double strand[46]). These include π-π, cation-π and anion-π interactions. Aromatic rings can interact with each other face-to-face (C···C) or edge-to-face (C-H···π).[47] The interactions can be either attractive or repulsive and this depends on the angle between aromatic rings and on their "offset" distance. Face-to-face stacking between two similar aromatic rings with non-offset at 0° degrees is repulsive and it becomes attractive as offset is increased. Alternatively, at non-offset and 90° edge-to-face is attractive and becomes repulsive when the CH edge moves from the π-system to the CH edge of the neighboring molecule.[3] This interaction is a "multicomponent" interaction and is composed of van der Waals, electrostatic, induction and charge-transfer interactions.[47] Induction and charge-transfer seem to have modest contribution to the stability of aromatic interactions. Solvophobic effect can further favour aromatic stacking as surfaces of π-electron systems are apolar. It has also been shown that it is fully possible to bind aromatic species (e.g., polycyclic aromatic hydrocarbons) via aromatic interaction by cyclophane.[48]

Cation-π interaction is in the simplest terms an electrostatic interaction. Cation interacts with the face of the π system (e.g., benzene). Strength of cation-π depends on charge density of cation and its hydration shell.[3] Also, anions can interact with electron-deficient aromatic systems.[16] This is mainly determined by electrostatic and ion-induced polarization. The negative quadrupole moment of benzene ring can be converted to positive by adding electron-withdrawing groups to the ring.[49,50] Such change makes otherwise unfavorable interaction between anion and π system favorable. Anion-π interactions can act as further stabilizing forces in receptor-anion complexation.[51]

2.2.5. Van der Waals

Van der Waals forces are non-directional and their contribution to receptor-anion binding ranges from weak to moderate. They are a form of electrostatic interaction that arises from the polarization of an electron cloud by the proximity of a neighboring nuclei. Because anions are highly polarizable and van der Waals forces relate to contact surface area of receptor and anion, the Van der Waals forces can be used to increase overall interaction energy between receptor and anion.

2.2.6. Solvophobic effect

Solvophobic effect is a phenomenon in highly polar media that causes species of low polarity to form aggregates to improve their solubility.[13] It is the strongest in water (where it is called hydrophobic effect) but it occurs also in other polar solvents or their mixtures with water. Hydrophobic effect is not a single interaction but a phenomenon relying simultaneously on different interactions. It is often one of the key driving forces in supramolecular complexation, especially in aqueous solutions. Hydrophobic effect strongly contributes to protein folding, membrane formation and small molecule binding in water.

When a hydrocarbon is dissolved in water it usually leads to increase in Gibbs free energy. Water-water interactions are very strong and have favorable ΔG change. Thus creating a cavity between water molecules for a nonpolar solute leads to increase of ΔG. As this process is exothermic,[52] entropy of the system must decrease. This occurs by water molecules forming a highly ordered structure around the hydrocarbon molecule and increase structuredness of the solvent. Aggregation of hydrocarbon molecules in water enables to free part of highly structured water molecules. This lowers the ordering influence of hydrophobic solutes and increases entropy ($\Delta S > 0$). Although, thermal energy ($\Delta H > 0$) is required for restructure of hydration shells around hydrocarbons, the free energy of system decreases upon aggregation ($\Delta G < 0$). This makes aggregation of hydrocarbon molecules in water a favorable process.[52] Because ΔH of aggregation is often small or even unfavorable, hydrophobic effect is generally entropy-driven.

2.3. Binding equilibria

Binding constants (K_{ass}) are one of the key measurands in characterizing binding process and express the thermodynamic stability of a supermolecule in a given solvent at a given temperature. K_{ass} values give direct quantitative information about sensitivity. Ratios of binding constants of the same host towards different guests give information about selectivity. K_{ass} is a thermodynamic parameter and is directly related to free energy of binding process ($\Delta G^{o} = -RT\ln K_{ass}$). This

means that binding affinity can be expressed for any given host-guest association reaction as K_{ass} or ΔG^{o} values.

Binding of a guest (G) to a host molecule (H) in 1:1 ratio with formation of complex (HG) can be described by equilibrium (2). The equilibrium constant K_{ass} expresses the affinity of a given host towards the guest. K_{ass} in equation (3) is expressed through activities of the species a_{HG}, a_H and a_G in the solution.

$$H + G \underset{}{\overset{K_{ass}}{\rightleftharpoons}} HG \tag{2}$$

$$K_{ass} = \frac{a_{HG}}{a_H a_G} \tag{3}$$

In dilute solutions K_{ass} can also be expressed via equilibrium concentrations of the species:

$$K_{ass} = \frac{[HG]}{[H][G]} \tag{4}$$

Determining the activity of the guest with high accuracy in the solvent can be difficult. In the context of anion binding possible sources for error can be ion-pairing[53] and homoconjugation[54]. Both of these processes can significantly affect the activity of the free anion. Quite often formally pure organic solvents are used as media. However, in any solvent there are always impurities, such as traces of water, that will strongly affect the solvation of anionic species[55] – and consequently also their activity. For solvents with low polarity this effect is especially strong.

Binding constant can be determined from experimental data via binding isotherm (see equation (5)).[13] It shows theoretical change in concentration of one components (complex) as a function of the concentration of the other component (host/guest) at a constant temperature.

$$[HG] = [H]_0 \frac{K_{ass} \cdot [G]}{1 + K_{ass} \cdot [G]} \tag{5}$$

This equation corresponds to 1:1 binding. [HG], $[H]_0$ and [G] are concentrations of host-guest complex, host and guest. The amount of host is kept constant and amount of guest is gradually increased while monitoring complex formation. Experimental methods (UV-vis, NMR, fluorescence, *etc.*) are usually used to monitor complex formation. There is a hyperbolic relationship between [HG] and [G] as [HG] concentration nears $[H]_0$. At high concentrations of guest the host will become saturated. Concentration level of guest necessary to saturate host depends on binding constant. The higher the binding affinity the less guest

is needed. Figure 1 shows how shape of isotherm changes upon the change in binding constant.

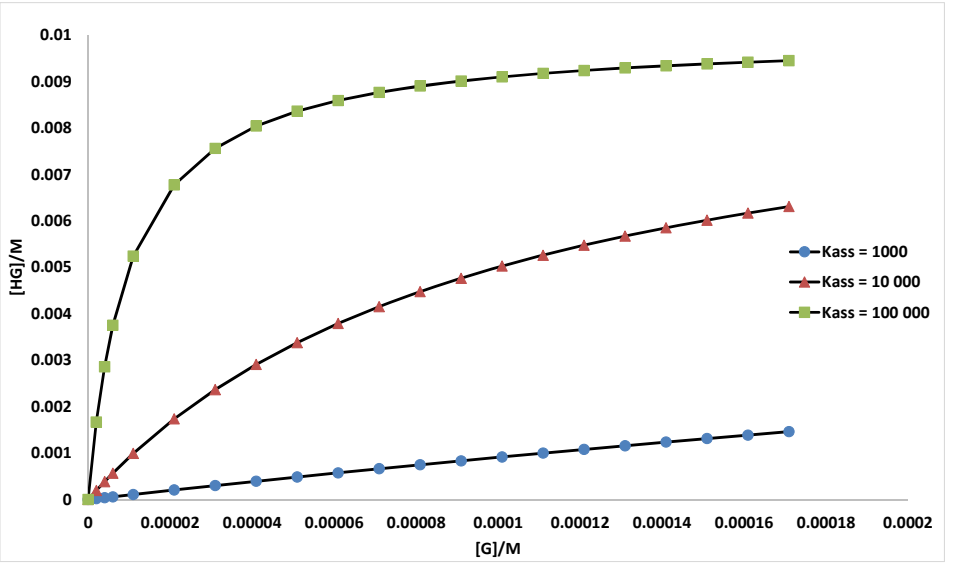

Figure 1. Binding isotherms for different K_{ass} with $[H]_0 = 0.01M$.

Treatment of non-linear binding data means generating a curve by minimizing the sum of squares of the vertical distances of the data points from the curve.[56] It requires computational approach to obtain binding constant data.

2.4. Solvent media

The molecular environment surrounding supramolecular complexes can affect not only the binding but also the structure of the formed supermolecule. Even energetically strong interactions can weaken greatly in the presence of solvent molecules. Solvent properties determine the solubility of the host, guest and host-guest complex. When host-guest complex has higher solubility than the individual species then binding is favored by the solvent. Anions have usually high solvation energies, and therefore, medium where binding constants are determined will strongly affect the results. Strongly solvated anions will have weaker interaction with the receptor and therefore, weaker binding. Important characteristics of solvents are dipole moment, electronic polarizability, hydrogen bond donor (HBD), hydrogen bond acceptor (HBA), electron pair donor (EPD) and electron pair acceptor (EPA) capability.[52] Specific solvation is caused solute/solvent association by hydrogen bonding or EPD/EPA interactions. Non-specific solvation is caused by polarizability in the solvent shell of dipolar solute molecules or ions. Under 1:1 binding stoichiometry two solvent cavities of host and guest become a single cavity which contains the complex. Standard

Gibbs free energy is dependent on the change in surface area as two species become one. Both host and guest are partially desolvated to come closer to each other. Solvation of formed complex releases solvent molecules from solvation shells of the host and the guest leading to increase in entropy (ΔS°) of the system.

Water is one of the most polar solvents (ε_r = 78.36)[52]. It is also, an amphiprotic solvent capable of strong self-association. Since water is strong HBD (α = 1.17)[57] and HBA (β = 0.47)[57], it solvates well both cations and anions. Water has good EPD and HPA capabilities (*DN* = 18 *AN* = 54.8).[57] Water is most widely used solvents and it is primary medium to molecular recognition in biological systems. Therefore, it is preferential to study receptor-anion interactions in water. Due to highly competitive nature of water the energetic effects of non-covalent interactions tend to be too weak to bind anionic species by synthetic receptors. Synthetic receptors also tend to have slow solubility in aqueous solutions which makes their use in water even more difficult.

Dimethyl sulfoxide (DMSO) is highly polar (ε_r = 46.71)[58] dipolar solvent. It has no HBD properties (α = 0.00)[57] and strong HBA ability (β = 0.76)[57]. It has good EPD and moderate EPA capability (DN = 29.8 *AN* = 19.3).[57] A large variety of both polar and non-polar compounds dissolve in DMSO. It is far less competitive than water making it a good medium for synthetic receptors to bind anions. Because DMSO is a HBA it can compete with anions to interact with HBD donor sites on neutral receptors. This weakens considerably binding compared to acetonitrile and chloroform. Still, good ability to dissolve different species and moderate competition make it a good medium to probe receptor-anion interactions.

Acetonitrile (AN) is similarly to DMSO an aprotic dipolar solvent with medium polarity (ε_r = 35.94)[58]. It has almost no acidic (α = 0.19)[57] and weak basic properties (β = 0.40)[57]. It has moderate EPD and EPA (*DN* = 14.1 *AN* = 18.9).[57] Low solvent competition makes binding interactions much higher than in more polar media. Somewhat more strict conditions for solvation narrow the range of receptors and anionic species that can be studied there.

Chloroform is apolar (ε_r = 4.89)[58] aprotic solvent. It is non-HBD and -HBA (α = 0.20, β = 0.10).[57] Chloroform is a weak EPD and moderate EPA (*DN* = 4.0 *AN* = 23.1)[57]. Ion-pairs can form readily in chloroform due to low charge separation. This makes ion-ion interaction much stronger in chloroform than in polar solvents. It solvates well apolar compounds and ion-pairs.

It is expected that binding constants increase in the following sequence: H_2O < DMSO < MeCN < $CHCl_3$.

2.5. Experimental techniques for studying supramolecular interactions

Binding constants are measured using experimental techniques by monitoring complex formation while changing concentration of the host or guest. From the perspective of basic methodology all binding constant determination methods are titrations where different experimental techniques are applied to detect changes in the sample composition (complex formation) during titrant addition. In order to have significant amounts of complexed and free host and guest in equilibrium state, a suitable concentration range must be used for experiment. This limits the range of binding constants that can be accurately measured with particular technique. Techniques with higher sensitivity usually have wider range and enable to measure higher binding constants.[59] Additionally, good distribution of titration points and saturation of the host by the guest are important for optimal accuracy. Best fit between experimental data and theoretical curve yields K_{ass} value.

UV-vis spectrophotometry

UV-Vis spectrophotometry relies on measuring the absorbance of the solution while adding the guest to the host or vice versa. Spectra at different ratios of unbound and bound host are recorded. It is essential that sample (host or guest) has absorbance maxima in visual or UV region. Also, there is an observable change in absorbance during complexation and titrant does not absorb in the analytical wavelength. Primary advantages of the method are its simplicity to use, robustness and good accuracy. High sensitivity enables K_{ass} determination in broad range (up to $10^6 \ldots 10^7$).[59]

Fluorescence

Fluorescence spectroscopy technique is similar to UV-vis spectrophotometry. Sample is excited at set absorbance maxima and during titration fluorescence emission intensity enhancement or quenching is observed at given wavelength. It is highly sensitive and enables to measure binding constant up to $10^7 \ldots 10^8$.[59] Main limitation to this method is that not all compounds possess fluorophores. Low emission efficiency can create the need to use higher concentrations, which can limit the binding constants that can be measured.

NMR spectrometry

Nuclear magnetic resonance (NMR) spectrometry is perhaps one of the most widely used methods in K_{ass} determination as people who prepare synthetic hosts are more familiar with this method in compound characterization. It provides both structural insights and binding constant data. Different signal detection modes are available and thus give different kind of output. Usually chemical

shifts of proton signals are used. This gives highest sensitivity and is easiest to use. Additionally, ^{13}C NMR can be used in conjunction with ^{1}H to yield better understanding of binding in the presence of multiple guests.[60] Host-guest equilibria can have fast or slow exchange rate compared with the NMR time scale.[59] Under most experimental conditions the receptor-anion equilibrium has fast exchange. Meaning, it is not possible to separate the signals of unbounds and bound receptor. In the spectrum averaged signal of both forms is observed. Low sensitivity of NMR limits binding constant range that can be determined with reasonable accuracy to 10^4.[59] The method requires higher concentrations which can also lead to undesired side processes.

Isothermal titration calorimetry ITC

Isothermal titration calorimetry (ITC) is a powerful tool for binding interaction characterization. It enables determination binding stoichiometry, binding constant and several thermodynamic parameters in a single titration. ITC has found good use especially in studying biochemical processes.[61,62] It involves measuring the heat impulses that are generated by the heat released or absorbed by the sample at a constant temperature during the titration. Registered signal is the sum total of all processes taking simultaneously place in the solution (including dilution, mixing, protonation/deprotonation). Presence of side processes or reactions can make data interpretation challenging. Measured heat is associated with forming and breaking of non-covalent bonds and is proportional to the enthalpy effect of the binding reaction. From the titration curve K_{ass}, also the standard molar Gibbs' free energy change ($\Delta G^o = -RT\ln K_{ass}$), can be found. Stoichiometry number n is used as an additional parameter, which corrects for impurity of titrant and errors in the presumed active volume of the cell.[63] Via the relation $\Delta G^o = \Delta H^o - T\Delta S^o$ the standard molar entropy change of the reaction can be found. Titration experiments at different temperatures enable also determination of the change in heat capacity (ΔC_p^o). A wide range of binding constant K_{ass} values, from 10^1 up to $10^8 \ldots 10^9$, can be measured.[64]

2.6. Neutral HB-based receptors

As said above, charged receptors can be pH sensitive and might only work in quite narrow pH window. Also, use of non-directional ion-ion interactions can lead to loss in selectivity. N-H fragments have become one of the primary choice in the design of neutral receptors that bind anionic species via hydrogen bonds.[15] Most of binding moieties are based on either pyrrole, amide and thioamide bonds or their combinations.[65] Hydrogen atom in N-H bond carries considerable partial positive charge, and therefore, has good hydrogen bond donicity. In receptor design HBD and acidity are important factors. In receptor chemistry low acidity and high HBD is desired. High acidity leads to proton transfer and deprotonation of receptor molecule. That results in loss in selectivity.

Because hydrogen bonding is preliminary process in acid-base reaction, it would be expected that higher HBD correlates with higher acidity. It has been found that such correlation may not exist.[66] Both the charge density of the donor and the acceptor affect the overall binding strength.[67] Scheme 2 shows molecular structures of frequently used HB donor groups of (thio)urea, carbazole, indole, pyrrole and indolocarbazole moieties.

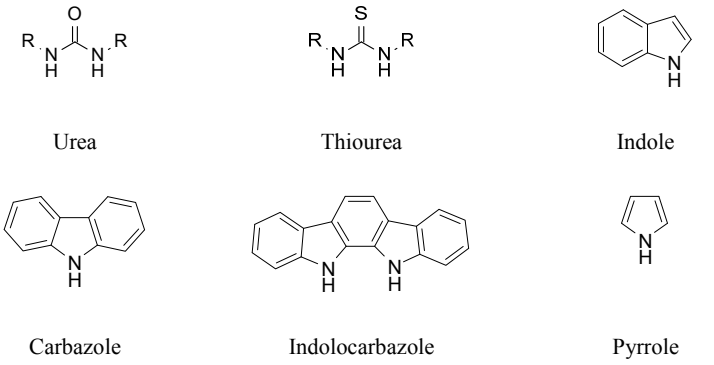

Scheme 2. Structures of HB donor groups

Ureas and thioureas are based on amide or thioamide bonds where two amino groups are connected by a carbonyl or thiocarbonyl group, respectively. In both cases there are two HBD N-H groups. With anions (thio)ureas are capable of forming bifurcated HBs with monoatomic guests and two single HBs with bidentate guests. Ability to form several HB enables to achieve stronger binding. This makes urea units excellent for carboxylate binding receptors.[68,69] Thioureas are around 6 pK_a units more acidic than urea counterparts in DMSO.[70] Addition of phenyl groups to urea moiety increases its acidity from 26.9 to 19.5 pK_a units in DMSO, making it even slightly more acidic than carbazole.[70] Receptors of different complexity have been prepared from ureas and thioureas.[71,72] Simplest are 1,3-diphenylurea receptors that can bind carboxylate anion in 1:1 stoichiometry by forming eight-membered ring.

Pyrrole is five-membered heterocyclic compound that contains one NH group. One pyrrole ring alone can form only one HB with an anion. By connecting several pyrrole ring together it is possible to build anion binding receptors for a large variety of anions. One of most frequent structures is calix[4]pyrrole that has shown great potential in binding monoatomic anions like chloride[73] or complex carboxylate based pharmaceuticals[74].

Carbazoles and indoles both contain pyrrole ring in their structure.[75] In a carbazole a benzene ring is fused to both sides of pyrrole forming a tricyclic structure. In case of indole only one benzene ring is fused to pyrrole. Both carbazole and indole contain a single NH group that can donate one hydrogen bond. Carbazole is around 1 pK_a unit more acidic than indole in DMSO.[70]

Indolocarbazole framework was first proposed by Beer and co-workers in 2005.[76] The molecule has rigid planar geometry where two pyrrole rings with

preorganized NH groups are connected by a benzene ring. This makes such structure perfect for designing a binding pocket for planar carboxylate anion. Reported acidity (pK_a) of indole, carbazole and pyrrole is 20.9, 19.9 and 23.0 in DMSO, respectively.[70] Indolocarbazoles have found use in simple substituted forms to foldamers.[75–77]

2.7. Carboxylate anions

Carboxylates are a diverse class of anionic compounds. They are key elements in biological systems. Carboxylates appear in different geometries, sizes, basicities, charges, *etc*. Based on the number of carboxylate groups in the compound they can be called mono-, di-, or tricarboxylates. Carboxylate group has distinct geometry where two oxygen atoms are attached to one carbon with equal CO bond lengths (1.26 Å in acetate) and bond angle between the CO bonds (120º in acetate).[78] The charge of carboxylate ions is largely localized on the oxygen atoms making these ions strongly solvated in HBD solvents and especially in water. The geometry of carboxylates enables to form hydrogen bonded complexes with chelating receptors in 1:1 stoichiometry. Although, carboxylate anions can be very different by structure, they still share similar carboxylic group. This means that two monocarboxylates with fairly different structure but similar basicity can be bound by the receptor with almost the same strength when interaction is mainly channeled through carboxylic group. As carboxylate group is similar to all carboxylates selective differentiation between carboxylates of similar basicity solely based on binding to carboxylate moiety is insufficient. It is vital to take into account geometrical aspects of the anion and its other properties (lipophobicity/lipophilicity, functional groups, *etc*.). Receptor design should aim to achieve optimal spatial arrangement to bind carboxylate group and incorporate secondary structural elements (additional HBD or HBA, aromatic/aliphatic substituents) to interact with carboxylate anion chain.

The more carboxylate groups an anion contains the more sophisticated receptor is needed to bind it selectively. Smallest and simplest of carboxylates are formate and acetate. Studying the binding of acetate to artificial receptors gives information of high value in predicting the binding of more complex carboxylates. Acetic acid, the conjugate acid of acetate has pK_a (water) = 4.76[78] and its $\log P_{\text{octanol-water}}$ = –0.17.[79] It is moderately strong acid and in neutral aqueous environment it is mainly in anionic form. Also, it is slightly lipophobic and is solvated quite strongly by water molecules. Therefore, acetate and other small carboxylates (benzoate, lactate, trimethylacetate) were chosen as initial study objects. From that point, it was possible to expand the selection towards carboxylates with larger diversity in hydrophobicity, geometry, basicity and size.

3. EXPERIMENTAL SECTION

3.1. Instruments and equipment

UV-vis spectrophotometric basicity measurements were performed in a MBraun Unilab glovebox with Perkin Elmer Lambda 40 and 45. Spectrometer was equipped with an external cuvette chamber via 2 optical cables that was in the glovebox. Spectra were recorded with bandwidth at 2 nm, scan speed at 240 nm/min and with 2 nm data recording interval.

UV-Vis spectrophotometric binding constant measurements were performed with Thermo Nicolet Evolution 300 spectrophotometer with Peltier-thermo-stated cell holders. The spectrophotometer was operated using the VisionPro 2.03 software. Scan speed was set to intelliscan mode. In the intelliscan mode the spectrophotometer changes the scan speed depending on how strongly the absorbance depends on the wavelength. Scan speed is varied from 120 nm/min to 1200 nm/min. When a peak is reached the scan speed is automatically reduced and after the peak the scan speed is increased again until the next peak is reached. Bandwidth was set at 1.5 nm and data recording interval to normal (1 nm).

Quartz cuvettes with 1 cm path length were used as sample and reference cuvettes. The sample cuvette was equipped with a PTFE-coated magnetic stirrer bar and closed with a plastic open-top screw-cap with PTFE-coated silicon septum.

Fluorescence spectrofluorometric measurements were carried out using Horiba FluoroMax-4 spectrofluorometer. Titration measurements were carried out in 1 cm quartz cells, using an excitation wavelengths between of 350 nm and 355 nm and recording emission spectra between 365 nm and 750 nm. The slit width for excitation and emission monochromators were 1 nm and 5 nm respectively. Titrations were carried out by monitoring the change in fluorescence intensity at the peak of the emission spectrum. ^{1}H NMR measurements were carried out on a 200 MHz NMR Bruker Avance II 200 NMR and 700 MHz NMR Bruker Avance II 700 NMR. Mettler Toledo DL 32 coulometric KF titrator was used to check water content in acetonitrile, DMSO and DMSO-d_6.

Solutions were prepared gravimetrically into borosilicate glass vials (4 ml and 15 ml). Compounds and solutions were weighed using Sartorius CPA225D-0CE analytical balance with digital resolution 0.00001 g. Dilutions of the solutions were made gravimetrically. Stock solutions were transferred to cuvette using Hamilton Gastight 50 µl and 100 µl syringes. Titration was carried out in the cuvette with Hamilton Gastight 100 µl syringes equipped with automatic dosage system (enabling reproducible dispensing of small volumes in 2 µl steps).

3.2. Chemicals

Bases and Receptors

Origin of studied bases are described in paper I. Most receptor molecules were synthesized and prepared in University of Tartu by colleague Sandip A. Kadam. Origin and synthesis of used receptors are described in papers II, III, IV, V and VI.

Anions

All anions were used in the form of tetrabutylammonium salts. Research included the following anions: acetate, trimethylacetate, benzoate, lactate, glyphosate and chloride. Commercially available Bu_4N^+ salts of acetate (Sigma Aldrich, 99%), benzoate (Sigma Aldrich, 99%) and chloride (Sigma Aldrich, ≥ 99.0%) were used. All others were prepared.

Anion Bu_4N^+ salts were prepared by mixing respective anion with 1 M $Bu_4N^+OH^-$ in methanol (Sigma Aldrich) in 1:1 molar ratio. TBA glyphosate salt was prepared in 2:1 molar ratio. The mixture was stirred for 24 h and dried under reduced pressure with rotary evaporator. Dried salts were stored in glovebox in argon atmosphere.

Solvents

Commercially available acetonitrile (HPLC for far UV/Gradient grade, J.T.Baker), DMSO (Sigma Aldrich, anhydrous ≥ 99.9%) and DMSO-d_6 (Deutero, 99.8%) were used. Work solvent for binding measurements was prepared by making a mixture of organic (acetonitrile, DMSO or DMSO-d_6) and water in 99.5:0.5 mass ratio.

3.3. Relative equilibrium constant measurements

For simplicity relative equilibrium constant measurements are described in the example of binding affinity measurements. In the case of acid-base equilibria guest (G) is the proton and H_1 and H_2 are acids (AH_1 and AH_2).
Binding equilibrium between two hosts towards a particular guest is described in equation (6). The relative binding affinity constant $\Delta\log K_{ass}$ is defined by equation (7).

$$H_1 + H_2G \xrightleftharpoons{\Delta\log K_{ass}} H_1G + H_2 \tag{6}$$

$$\Delta \log K_{ass} = \log K_{ass}(H_1G) - \log K_{ass}(H_2G) = \log \frac{a_{H_1G} a_{H_2}}{a_{H_2G} a_{H_1}} \tag{7}$$

In context of receptor binding, activity of anion, which is strongly affected by solvent and other dissolver species, becomes unnecessary. Side-proccesses associated with anion acitivity, e.g., ion-pairing and homoconjugation, influence both receptor complexation processes simultaneously and to similar extent and cancel out. Additional influencing variables like solvent composition, temperature and other experimental conditions are identical for both receptors. Assumption that the ratios of activity coefficients of γ(H)/γ(HG) are similar for the different receptor molecules is made. Equation (8) is derived then by replacing ratios of activities in equation (7) by equilibrium concentrations.

$$\Delta \log K_{\text{ass}} = \log K_{\text{ass}}(\text{H}_1\text{G}) - \log K_{\text{ass}}(\text{H}_2\text{G}) = \log \frac{[\text{H}_1\text{G}][\text{H}_2]}{[\text{H}_2\text{G}][\text{H}_1]} \qquad (8)$$

3.3.1. UV-vis spectrophotometric measurements

All solutions were prepared gravimetrically into vials. For ease of titration, titrants with two concentrations were used. Titrant with lower concentration was used in the beginning and with higher concentration at the end to ensure full complexation. Spectrophotometric titrations were carried out at (25 ± 0.1) °C. Binding affinity measurements solution preparation and procedures are described in II and III. The experimental setup and pK_a measurement method is same as used previously.[54,80]

In order to determine relative binding affinity via spectrophotometric method, it is necessary to measure, also, the spectra of free receptor and fully complexed receptor-anion forms of both receptors. Firstly, both titration absorption spectra for both receptors were registered. Secondly, titration absorption spectra of mixture containing both receptors at different complexation levels were registered. H_1 and H_2 were chosen, which had sufficiently different spectra and similar binding affinity ($\Delta\log K_{\text{ass}} < 1$). Dissociation level α of a receptor-anion complex can be defined in the following way:

$$\alpha = \frac{[\text{H}]}{[\text{H}] + [\text{HG}]} = \frac{A^{\lambda} - A^{\lambda}_{\text{HG}}}{A^{\lambda}_{\text{H}} - A^{\lambda}_{\text{HG}}} \qquad (9)$$

A^{λ} is absorbance at a particular titration step, A^{λ}_{H} and A^{λ}_{HG} are the absorbances of the free receptor and receptor-anion complex, respectively. According to equation (25) from the spectra of the mixture the degrees of dissociation for both receptor-anion complexes were found using multilinear regression. $\Delta\log K_{\text{ass}}$ value was calculated according to equation (10). Both measurement and calculation method bear similarities to the one used earlier by our group for pK_a measurements in nonaqueous solvents.[54,81] By replacing the

equilibrium concentration in equation (8) with α_1 and α_2, which are the degrees of dissociation of H_1G and H_2G, $\Delta\log K_{ass}$ values were found using following equation:

$$\Delta\log K_{ass} = \log\frac{\alpha_2(1-\alpha_1)}{(1-\alpha_2)\alpha_1} \tag{10}$$

$\Delta\log K_{ass}$ values are calculated at each titration point by finding from spectral data the degrees of dissociation of the receptor-anion complexes as defined by equation (10) for both receptors H_1 and H_2. The optical path length l is equal for all compounds and is taken into account in A^{λ}. Absorbance caused by solvent is compensated by solvent blank in the reference cuvette.

According to Lambert-Beer's law the absorbance A^{λ} of a species X in a solution with unit path length at wavelength λ can be expressed by the following equation:

$$A_X^{\lambda} = \varepsilon_X^{\lambda}[X] \tag{11}$$

where ε_X^{λ} is the molar extinction coefficient of X at given wavelength λ and [X] is the concentration of X in the solution. In a situation where the solution contains two partially dissociated receptor-anion complexes H_1G and H_2G, and the anion G does not absorb, the absorbance can be expressed as follows:

$$A^{\lambda} = \varepsilon_{H_1G}^{\lambda}[H_1G] + \varepsilon_{H_1}^{\lambda}[H_1] + \varepsilon_{H_2G}^{\lambda}[H_2G] + \varepsilon_{H_2}^{\lambda}[H_2] \tag{12}$$

By taking the sum of the equilibrium concentrations of free receptor and receptor-anion complex as unity the equilibrium concentrations of receptor-anion complexes can be expressed via normalized concentrations:

$$[H_1G] = 1 - [H_1] \text{ and } [H_2G] = 1 - [H_2] \tag{13}$$

Equation (12) can modified in the following way:

$$A^{\lambda} = \varepsilon_{H_1G}^{\lambda} + \varepsilon_{H_2G}^{\lambda} + (\varepsilon_{H_1}^{\lambda} - \varepsilon_{H_1G}^{\lambda})[H_1] + (\varepsilon_{H_2}^{\lambda} - \varepsilon_{H_2G}^{\lambda})[H_2] \tag{14}$$

If there are only free receptor forms in the solution then equation (14) simplifies into the following form:

$$A^{\lambda} = [H_1]\varepsilon_{H_1}^{\lambda} + [H_2]\varepsilon_{H_2}^{\lambda} \tag{15}$$

The terms on the right side of this equation can be expressed through absorbances of pure compounds in free receptor form multiplied by coefficients c_1 and c_2, which are the ratios of concentrations of H_1 and H_2 in mixture and solution of pure compounds. When both receptor molecules are not bound to the anion, then via normalized concentrations $[H_1] = 1$ and $[H_2] = 1$ values can be expressed:

$$\varepsilon^{\lambda}_{H_1} = c_1 A^{\lambda}_{H_1\,pure} \tag{16}$$

$$\varepsilon^{\lambda}_{H_2} = c_2 A^{\lambda}_{H_2\,pure} \tag{17}$$

Coefficients c_1 and c_2 are constant over the wavelength range while taking into account the assumption that $\varepsilon^{\lambda} \neq 0$. By combining equations (15), (16) and (17) it is possible to calculate coefficients c_1 and c_2 from the spectrum of mixture of compounds in free receptor form and from the spectra of both pure compounds in free receptor form by minimizing the least squares over the chosen wavelength range:

$$S_p = \sum_{\lambda} (A^{\lambda} - c_1 A^{\lambda}_{H_{1pure}} - c_2 A^{\lambda}_{H_{2pure}})^2 \tag{18}$$

Similarly to equation (15), if both receptor molecules are in the form of receptor-anion complex, absorbance of the mixture can be written:

$$A^{\lambda} = [H_1G]\varepsilon^{\lambda}_{H_1G} + [H_2G]\varepsilon^{\lambda}_{H_2G} \tag{19}$$

By also taking into account normalized concentrations, the ε^{λ} values on the right side of equation (19) can be written:

$$\varepsilon^{\lambda}_{H_1G} = c_1 A^{\lambda}_{H_1G\,pure} \tag{20}$$

$$\varepsilon^{\lambda}_{H_2G} = c_2 A^{\lambda}_{H_2G\,pure} \tag{21}$$

The degrees of dissociation α_1 and α_2 of receptor-anion complexes H_1G and H_2G can be introduced into equation (14), as well as the ratios of concentrations c_1 and c_2 and the absorbances of the pure forms by using equations (16), (17), (20) and (21):

$$A^{\lambda} = c_1 A^{\lambda}_{H_1G\,pure} + c_2 A^{\lambda}_{H_2G\,pure} + \alpha_1 c_1 (A^{\lambda}_{H_1\,pure} - A^{\lambda}_{H_1G\,pure}) + \alpha_2 c_2 (A^{\lambda}_{H_2\,pure} - A^{\lambda}_{H_2G\,pure}) \tag{22}$$

Equation (22) can be rewritten as a two-parameter linear regression model for calculating α_1 and α_2:

$$A^{\lambda} - c_1 A^{\lambda}_{\mathrm{H_1G\,pure}} - c_2 A^{\lambda}_{\mathrm{H_2G\,pure}} = \alpha_1 c_1 (A^{\lambda}_{\mathrm{H_1\,pure}} - A^{\lambda}_{\mathrm{H_1G\,pure}}) + \alpha_2 c_2 (A^{\lambda}_{\mathrm{H_2\,pure}} - A^{\lambda}_{\mathrm{H_2G\,pure}}) \quad (23)$$

Least squares minimization is used for S_s over given wavelength range to find α_1 and α_2 at different anion concentration levels:

$$S_s = \sum_{\lambda} [A^{\lambda} - c_1 A^{\lambda}_{\mathrm{H_1G\,pure}} - c_2 A^{\lambda}_{\mathrm{H_2G\,pure}} - \\ - \alpha_1 c_1 (A^{\lambda}_{\mathrm{H_1\,pure}} - A^{\lambda}_{\mathrm{H_1G\,pure}}) - \alpha_2 c_2 (A^{\lambda}_{\mathrm{H_2\,pure}} - A^{\lambda}_{\mathrm{H_2G\,pure}})]^2 \quad (24)$$

Additionally, intercept b_0 can be introduced and the following three-parameter regression can be used:

$$A^{\lambda} - c_1 A^{\lambda}_{\mathrm{H_1G\,pure}} - c_2 A^{\lambda}_{\mathrm{H_2G\,pure}} = \\ = \alpha_1 c_1 (A^{\lambda}_{\mathrm{H_1\,pure}} - A^{\lambda}_{\mathrm{H_1G\,pure}}) + \alpha_2 c_2 (A^{\lambda}_{\mathrm{H_2\,pure}} - A^{\lambda}_{\mathrm{H_2G\,pure}}) + b_0 \quad (25)$$

Equations (23) and (25) give usually similar results. Equation (25) can take into account slight baseline shifts that have occurred between the measurements of spectra of pure compounds and mixture.

3.3.2. ^{1}H NMR spectrometric measurements

^{1}H NMR experiments were carried out at 25°C under fast exchange conditions. In more detail the description of the procedure is described in publications III and IV. General pathway of the method entailed titrating a mixture of receptors (2 or more) with the anion titrant. First, the ^{1}H NMR spectrum of the mixture was recorded. From the spectrum signals corresponding to NH protons of the receptors where identified. During binding of anion to receptor molecules the NH protons are deshielded and move left on the spectrum. Spectra of complexation were recorded throughout the experiment till full complexation of all receptor molecules was observed. On average 16–18 spectra were recorded during the titrations. From the shifts of the chemical signals the degrees of complexation β of respective receptor-anion complexes were calculated (see equation (26)).

$$\beta = \frac{[\mathrm{H_x}]}{[\mathrm{H_x}] + [\mathrm{H_xG}]} = \frac{\delta - \delta_{\mathrm{H_x}}}{\delta_{\mathrm{H_xG}} - \delta_{\mathrm{H_x}}} \quad (26)$$

δ is chemical shift at the titration step, δ_{H_x} and δ_{H_xG} are the chemical shifts of free receptor molecule and receptor-anion complex, respectively. By replacing the equilibrium concentrations in equation (8) with the association degrees of H_1 and H_2, β_1 and β_2, the $\Delta\log K_{ass}$ values are found using the following equation:

$$\Delta\log K_{ass} = \log\frac{\beta_1(1-\beta_2)}{(1-\beta_1)\beta_2} \tag{27}$$

3.4. Absolute logK_{ass} measurements

Measurement procedures of absolute $\log K_{ass}$ values are described in publication II. The working conditions and solvents used were largely the same as used in the measurements of relative binding constants. The absorption spectra of the free receptor, fully complexed receptor and spectra at different complexation levels were recorded. Amounts of added anion where determined by weighing the measurement cuvette after each addition of the titrant. Over the course of titration around 14–18 spectra were recorded. Three methods were used for calculation of the binding constants. The assigned binding constant values for each run were averaged from the results of the three calculation methods taking into account their internal consistency.

Calculation from every individual titration point: equation (4) was modified by replacing equilibrium concentrations of free receptor and receptor-anion complex through α to obtain the equation for finding the $\log K_{ass}$ values:

$$\log K_{ass} = \log\frac{(1-\alpha)\cdot\gamma_{HG}}{\alpha\cdot[A^-]\cdot\gamma_G} \tag{28}$$

γ_{HG} and γ_G are the activity coefficients of receptor-anion complex and the anion of interest respectively. The activity coefficients were calculated according to the Debye-Hückel equation:

$$\log\gamma = -\frac{Az^2\sqrt{I}}{1+Ba\sqrt{I}} \tag{29}$$

A and B are solvent dependent constants, I is the ion strength, z the ion charge and a the effective ion radius in solution. A and B values for MeCN are 1.64 and 0.48 and for DMSO are 1.12 and 0.43.[82]

Least square fitting of the isotherm, without linearization: based on equations (3) and (9) it is possible to arrive at the equation of the binding isotherm:

$$\Delta A = \Delta A_{\max} \frac{K_{\text{ass}} \cdot \frac{[\text{A}^-]\gamma_{\text{G}}}{\gamma_{\text{HG}}}}{1 + K_{\text{ass}} \cdot \frac{[\text{A}^-]\gamma_{\text{G}}}{\gamma_{\text{HG}}}} \tag{30}$$

, where ΔA equals $A^{\lambda} - A_{\text{H}}^{\lambda}$. K_{ass} was found by fitting the experimental data to this isotherm using the least squares approach and taking $\Delta A_{\max}$ (equal to $A_{\text{HG}}^{\lambda} - A_{\text{H}}^{\lambda}$) and K_{ass} as adjustable parameters.

Least square fitting of the isotherm, with linearization: the equation (30) was linearized as described by Benesi and Hildebrand[83] to arrive at the following equation:

$$\frac{1}{A^{\lambda} - A_{\text{H}}^{\lambda}} = \frac{\gamma_{\text{HG}}}{K_{ass}(A_{\text{HG}}^{\lambda} - A_{\text{H}}^{\lambda})[\text{A}^-]\gamma_{\text{G}}} + \frac{1}{A_{\text{HG}}^{\lambda} - A_{\text{H}}^{\lambda}} \tag{31}$$

By plotting $\frac{1}{A^{\lambda} - A_{\text{H}}^{\lambda}}$ vs $\frac{\gamma_{\text{HG}}}{[\text{A}^-]\gamma_{\text{G}}}$ graph K_{ass} can be found from the slope.

3.5. Obtaining absolute logK_{ass} from relative logK_{ass} values

Anion binding scales were created from relative binding constants, where each arrow on the scale represents a measurement between two receptors. The scales of relative binding affinity were anchored to directly measured absolute logK_{ass} values (anchor points) by least squares procedure. The logK_{ass} values for individual receptors from relative binding affinity measurements were found by minimizing the sum of squares of the differences between the directly measured $\Delta\log K_{\text{ass}}$ values and the assigned logK_{ass} values, which is denoted as *SS* in the following equation:

$$SS = \sum_{i=1}^{n_m} \left\{ \Delta\log K_{\text{ass}}^{\text{i}} - \left[\log K_{\text{ass}}(\text{H}_2\text{G}) - \log K_{\text{ass}}(\text{H}_1\text{G}) \right] \right\}^2 \tag{32}$$

The sum is taken over the measurements between all receptors included in the binding scale. Every $\Delta\log K_{\text{ass}}^{\text{i}}$ value is the directly measured relative binding strength of the receptors H_1 and H_2 (H_2 has higher logK_{ass} value). The absolute

$\log K_{ass}$ value for each receptor in the scale is calculated by the least squares procedure. The consistency of the results – the goodness of match between the assigned absolute $\log K_{ass}$ values and the measured $\Delta\log K_{ass}$ values – can be assessed by the consistency standard deviation *s*, which is found according to the following equation:

$$s = \sqrt{\frac{SS}{n_m - n_c}} \tag{33}$$

, where n_m is the total number of $\Delta\log K_{ass}$ value measurements and n_c is the number of absolute $\log K_{ass}$ values that were determined. This value can be regarded as an average reproducibility standard deviation of the $\Delta\log K_{ass}$ measurements. Consistency of the measurements of $\Delta\log K_{ass}$ values can be assessed by consistency parameter *s*. However, this parameter characterizes the whole binding scale and does not express the uncertainties of the individual $\log K_{ass}$ values of receptor molecules on the scale. Uncertainty estimation using the classical ISO GUM modeling approach is difficult because of the difficulties in quantization of different uncertainty sources (side-reactions, determination of activity coefficients, impurities).[81] Therefore a simpler approach was used and the uncertainty of the $\log K_{ass}$ values can be found according to the following equation:

$$u_c(\log K_{ass})_x = \sqrt{u(\sum \Delta \log K_{ass})^2 + u(anchoring)^2 + u(sys)^2} \tag{34}$$

, where $u(\sum\Delta\log K_{ass})$ expresses the random effect in $\Delta\log K_{ass}$ measurements, *u*(anchoring) expresses the random effect in anchoring the scale and *u*(sys) expresses the systematic effect in measurement of absolute $\log K_{ass}$ values of the anchor compounds. $u(\sum\Delta\log K_{ass})$ is the standard deviation of arithmetic mean of $\Delta\log K_{ass}$ value measurements with an individual receptor molecule. *u*(anchoring) is found as root mean square (RMS) of differences between directly measured $\log K_{ass}$ values of the anchoring compounds and values obtained from the scale. *u*(sys) is a subjective estimation based on the long-term experience with similar measurements in our group.

The uncertainties of the absolute $\log K_{ass}$ values were calculated in two ways. The first was based on the uncertainties of the $\Delta\log K_{ass}$ value measurements only (second and third members in equation (34) were regarded zero). The second way includes also the random effect in anchoring of the scale and the systematic effect in the determination of absolute $\log K_{ass}$ values. The uncertainties obtained using the first way describe how accurately is it possible to measure $\log K_{ass}$ values using the relative binding constant approach and are the appropriate uncertainty estimates to use when comparing the $\log K_{ass}$ values of different compounds on the scale. The uncertainty obtained via the second approach estimates, how accurately is it possible to obtain the absolute binding

constant values as thermodynamic equilibrium constant values in the used solvent. These uncertainties are appropriate to use when comparing the absolute logK_{ass} values from this work with those from other research groups.

3.6. Continuous variation method (Job plot method)

Stoichiometry of binding interaction was determined via Job plot method.[84] The mole fractions of the receptor and anion are changed while keeping the sum of molar concentrations constant. Absorption in UV-vis spectrum was measured to monitor the formation of the complex. Anion mole fraction was varied from 0.1 to 0.9 with 0.1 step. Complex formation was plotted against anion mole fraction. The stoichiometry was obtained from x-coordinate at the maximum of the curve at y-axis. As the result of described method is sensitive towards inputs care should be taken when interpreting reaction stoichiometry.[85]

Results of Job plot analysis are presented in Table 1. It was confirmed that for small receptor molecules like substituted indolocarbazoles or diphenylureas binding between carboxylates takes place in 1:1 ratio. Receptors prepared for glyphosate in paper VI showed, except for receptors **16** and **17**, 1:1 binding ratio with Gly^{2-}. Still at low concentration even **16** and **17** could be plotted with 1:1 binding isotherm, which is more desired as in practical applications anion concentrations tend to be quite low.

Table 1. Binding ratios estimated from Job plot analysis

Receptor	**Anion**[a]	**Binding ratio**	**Solvent medium**
Indolocarbazole (Indolo[2,3-a]carbazole)	Acetate	1:1	MeCN:H_2O (99.5%:0.5% m/m)
4-CF3-phenylthiourea	Acetate	1:1	MeCN:H_2O (99.5%:0.5% m/m)
3,4,4′-Cl3-diphenylurea	Acetate	1:1	MeCN:H_2O (99.5%:0.5% m/m)
Gly^{2-} Receptor **2**	Glyphosate dianion	1:1	DMSO:H_2O (99.5%:0.5% m/m)
Gly^{2-} Receptor **3**	Glyphosate dianion	1:1	DMSO:H_2O (99.5%:0.5% m/m)
Gly^{2-} Receptor **4**	Glyphosate dianion	1:1	DMSO:H_2O (99.5%:0.5% m/m)
Gly^{2-} Receptor **5**	Glyphosate dianion	1:1	DMSO:H_2O (99.5%:0.5% m/m)
Gly^{2-} Receptor **6**	Glyphosate dianion	1:1	DMSO:H_2O (99.5%:0.5% m/m)
Gly^{2-} Receptor **8**	Glyphosate dianion	1:1	DMSO:H_2O (99.5%:0.5% m/m)
Gly^{2-} Receptor **10**	Glyphosate dianion	1:1	DMSO:H_2O (99.5%:0.5% m/m)
Gly^{2-} Receptor **12**	Glyphosate dianion	1:1	DMSO:H_2O (99.5%:0.5% m/m)
Gly^{2-} Receptor **13**	Glyphosate dianion	1:1	DMSO:H_2O (99.5%:0.5% m/m)
Gly^{2-} Receptor **14**	Glyphosate dianion	1:1	DMSO:H_2O (99.5%:0.5% m/m)
Gly^{2-} Receptor **16**	Glyphosate dianion	1:2	DMSO:H_2O (99.5%:0.5% m/m)
Gly^{2-} Receptor **17**	Glyphosate dianion	1:2	DMSO:H_2O (99.5%:0.5% m/m)

[a] anions were used in the form of TBA salts.

4. RESULTS

4.1. Development of relative equilibrium constant measurement methods

Equilibrium constant measurement can be performed by measuring it directly according to equilibrium (2). Then it becomes necessary to measure the activities of all species involved in the reaction. With some species this can be challenging and introduce a variety of measurement uncertainties. An alternative approach is to measure relative equilibrium constants, see equation (6). In the present work it was applied in basicity study of phosphanes and receptor-anion binding interactions. In non-aqueous environments accurate quantification of proton activity in acid-base reactions is difficult and therefore relative measurements, which eliminate the necessity to measure proton's activity, are advantageous. Similarly, binding interactions in host-guest systems involve measurement of free substrate activity. This can be influenced by temperature, solvent composition and side reaction (homoconjugation, ion-pairing). As can be seen in equation (6) and in equation (7), there is no need to measure guest's activity in the case of relative measurement approaches.

UV-Vis spectrophotometric relative acidity/basicity measurement method

Spectrophotometric relative pK_a measurement method was applied to study the basicities of 4 phosphanes and 6 diphosphanes in acetonitrile. Results of ΔpK_a measurements are presented in Table 2. Measurements involved determining relative acidities of two conjugate acids B_1H^+ and B_2H^+ of bases B_1 and B_2. Basicity of a base B be can be expressed through the negative logarithm of dissociation constant pK_a of its conjugate acid BH^+.[86] Analogous methods have been described and applied for a series of acid-base measurements.[54,81] Based of all relative pK_a measurements a relative basicity scale in respective solvent medium is composed. Each arrow on the scale represents the result of one experimental relative measurement series. Absolute pK_a values for measured bases are found by anchoring them to absolute pK_a value of pyridine (pK_a value 12.53).[80] High precision of such measurements makes it possible to compare similar basicities.

Measured pK_a values enable studying the trends in basicity of methyl- and phenyl-substituted phosphanes and amines in acetonitrile (see Sheme 3). Aryl-substituted phosphanes are weaker based than alkyl-substituted phosphanes. This is mainly caused by weak conjugation between the aromatic ring and the lone pair of the phosphorus atom in the neutral phosphane and by the field inductive effect of the aromatic ring. Amines experience much larger decrease in basicity when a methyl group is substituted for a phenyl group, first of all caused by the much larger penalty due to the resonance-stabilization of the neutral.

Table 2. Results of the basicity measurements of phosphanes in acetonitrile.[a]

	Base	pK_a	ΔpK_a	pK_a[b] (literature)	difference
A1	2-NO_2-4-CF_3-$C_6H_3P_1$(pyrr)	16.54			
A2	2-amino-1-methylbenzimidazole	16.31			
A3	2-aminobenzimidazole	16.08			
A4	**1,2-bis(dimethylphosphino)ethane**	**15.6**			
A5	**Trimethylphosphine**	**15.5**		16.6	-1.1
A6	2,4,6-trimethylpyridine	14.98			
A7	2-methylpyridine	13.32			
A8	**Dimethylphenylphosphine**	**12.69**		13.7	-1.01
A9	Pyridine	12.53			
A10	2-methylkinolin-8-amine	11.54			
A11	2-methoxyaniline	10.50			
A12	5-NO_2-benzimidazole	10.39			
A13	**1,4-bis(diphenylphosphino)butane**	**10.22**			
A14	**Tris(4-methoxyphenyl)phosphine**	**10.06**		11.2	-1.14
A15	2-methoxypyridine	9.93			
A16	**1,3-bis(diphenylphosphino)propane**	**9.83**			
A17	1-naphtylamine	9.77			
A18	**1,2-bis(diphenylphosphino)ethane**	**9.37**			
A19	2,4-difluoroaniline	8.39			
A20	**1,4-bis(diphenylphosphino)butaneH+**	**8.3**			
A21	**BIPHEP**	**7.98**			
A22	2-Cl-aniline	7.86			
A23	**BINAP**	**7.80**			
A24	2,6-dimethoxypyridine	7.64			
A25	**Triphenylphosphine**	**7.64**		8.8	-1.16
A26	**1,3-bis(diphenylphosphino)propaneH+**	**7.4**			
A27	2-Cl-pyridine	6.79			
A28	**N-methyldiphenylamine**	**6.52**			
A29	4-NO_2-aniline	6.22			
A30	2,5-dichloroaniline	6.21			
A31	**1,2-bis(diphenylphosphino)ethaneH+**	**5.8**			
A32	2,6-dikloroaniline	5.06			
A33	2-NO_2-aniline	4.80			
A34	**BIPHEPH+**	**4.0**			
A35	4-Cl-2-NO_2-aniline	3.80			
A36	**BINAPH+**	**3.8**			
A37	**2-Cl-4-NO_2-aniline**	**3.66**			
A38	**5-Cl-2-NO_2-aniline**	**3.22**			
A39	**2,3,5,6-tetrachloroaniline**	**2.73**			
A40	**2,3,4,5,6-pentachloroaniline**	**2.35**			
A41	**Triphenylamine**	**1.3**			

[a] Bases investigated in this work are given in bold, the remaining bases are the reference bases. [b] pK_a values from literature.

$$\underset{pK_a = 7.64}{PPh_3} \leftarrow 2.32 \rightarrow \underset{pK_a = 9.96^{[80]}}{Ph_2PMe} \leftarrow 2.73 \rightarrow \underset{pK_a = 12.69}{PhPMe_2} \leftarrow 2.81 \rightarrow \underset{pK_a = 15.5}{PMe_3}$$

$$\underset{pK_a = 1.3}{NPh_3} \leftarrow 5.22 \rightarrow \underset{pK_a = 6.52}{Ph_2NMe} \leftarrow 4.91 \rightarrow \underset{pK_a = 11.43^{[80]}}{PhNMe_2} \leftarrow 6.18 \rightarrow \underset{pK_a = 17.61^{[87]}}{NMe_3}$$

Scheme 3. Basicity trend of methyl- and phenyl-substituted phosphanes and amines in acetonitrile.

Also, basicities of 5 monoprotonated diphosphanes were characterized. Protonation of the first phosphorus significantly lowers the basicity of the second basicity center. This is caused by the inductive effect of the protonated basicity center and the electrostatic repulsion of the positive charges. The closer the basicity centers are, the stronger is the repulsion effect (e.g., BINAP and BIPHEP).

UV-Vis spectrophotometric relative binding affinity measurement method

Relative binding affinity measurement bears similarities to relative acidity measurement. UV-vis spectrophotometric binding affinity measurement method involves the measurement of change in absorbance during anion addition. It requires that host (receptor) absorbs in visual or UV region and the complexed form has different absorbance spectrum from free host.

Through this a series of spectra are recorded of solutions containing unbound and bound receptor at different ratios. In relative binding affinity measurement method two receptors are dissolved in the same solution. The absorbance of the solution at a given wavelength is the sum of all the species present in the solution. This introduces a challenge as spectral overlap is very common in UV-vis spectrophotometry. In ideal case the absorbance maxima of the two receptors are positioned separately. Then it would be possible to find the degrees of dissociation/association of the complex for both receptors from spectral changes corresponding to the individual species. Figure 2 is a schematic of determination of $\Delta \log K_{ass}$ value.

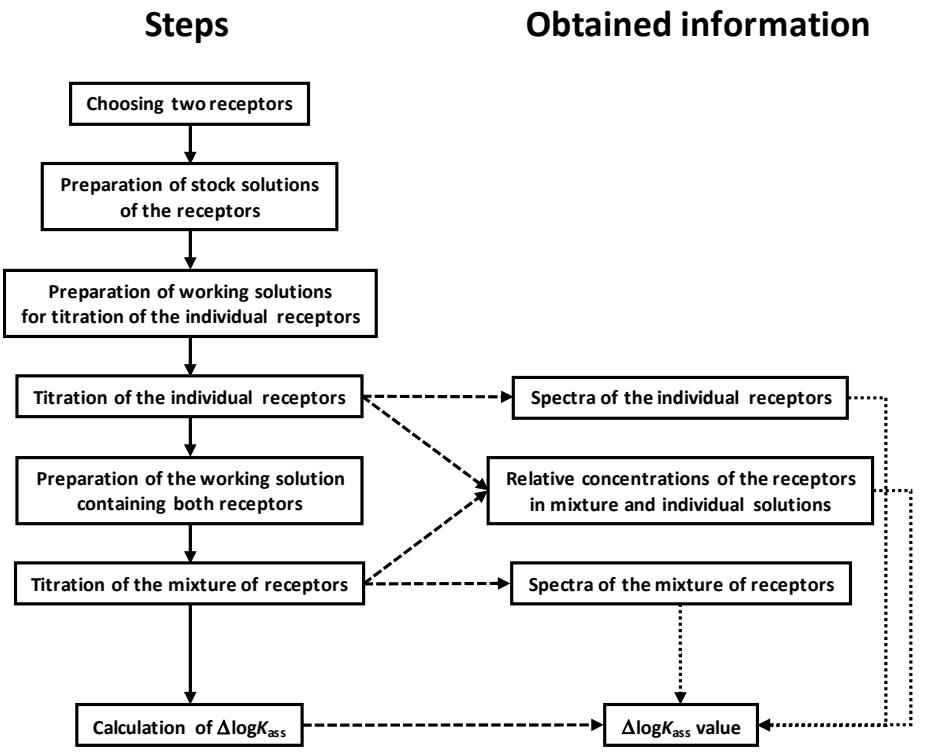

Figure 2. Flowchart of $\Delta\log K_{ass}$ value measurement.

In the current context spectral overlap leads to necessity of more complex data treatment that was explained in section 3.3. Measurement method involves titration of individual species and mixture of the receptors (see Figure 3). Degrees of dissociation of the receptor-anion complexes are found via a least squares minimization process. Relative binding affinities ($\Delta\log K_{ass}$) are found according to equation (10).

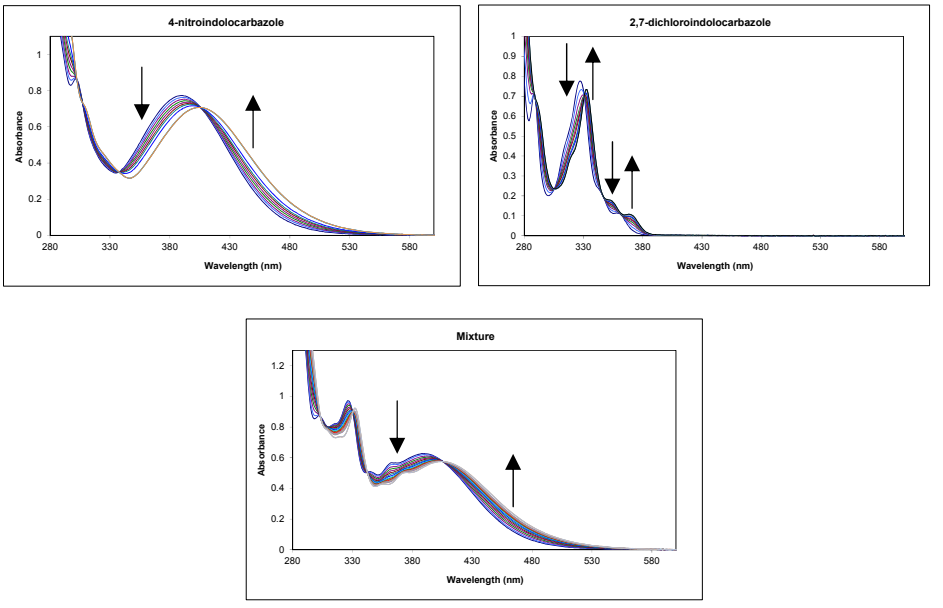

Figure 3. Titration spectra of UV-vis relative binding affinity measurement between 4-NO_2-indolocarbazole and 2,7-Cl_2-indolocarbazole towards acetate.

By measuring a number of different receptors against the same anion a scale of anion binding can be constructed. Method development was carried out with 28 indolocarbazole- and (tio)urea-based receptors towards acetate anion. Acetate was chosen a probing anion to develop and test the measurement method. Relative binding affinities alongside with assigned absolute binding constant values of synthetic receptors towards acetate are presented in Table 3. Absolute binding constants ($\log K_{ass}$) along with estimated standard uncertainties were assigned to each receptor using the procedures described in section 3.5. The relative binding scale is anchored to absolute binding constant values of indolocarbazole and 1,10-dichloroindolocarbazole. Each receptor on the scale has been measured against at least two partners.

Table 3. Self-consistent scale of acetate binding in acetonitrile (99.5% : 0.5% m/m).[a]

No	Receptor molecule	logK_{ass}	u_c[b]	u_c[c]	ΔlogK_{ass}
22	1,3-bis(4-nitrophenyl)urea	**6.04**	**0.04**	**0.05**	
5	4-NO_2-indolocarbazole	**5.24**	**0.04**	**0.05**	
23	3,4,4′-Cl_3-diphenylurea	**5.20**	**0.02**	**0.04**	
16	4,7-Cl_2-indolocarbazole	**5.20**	**0.03**	**0.04**	
4	2-NO_2-indolocarbazole	**5.09**	**0.00**	**0.03**	
15	2,7-Cl_2-indolocarbazole	**5.05**	**0.01**	**0.04**	
14	2,9-Cl_2-indolocarbazole	**4.95**	**0.02**	**0.04**	
17	1-(4-nitrophenyl)-3-hexylthiourea	**4.70**	**0.02**	**0.04**	
26	1-(4-nitrophenyl)-2-thiourea	**4.69**	**0.02**	**0.04**	
9	2-MeO-indolocarbazole	**4.50**	**0.02**	**0.04**	
8	4,7-$(MeO)_2$-indolocarbazole	**4.48**	**0.01**	**0.03**	
1	**Indolocarbazole**	**4.46**	**0.01**	**0.03**	
7	2,7-$(MeO)_2$-indolocarbazole	**4.46**	**0.02**	**0.04**	
18	1-(4-CN-phenyl)-3-hexylthiourea	**4.44**	**0.02**	**0.04**	
2	5,6-dihydroindolocarbazole	**4.36**	**0.00**	**0.03**	
21	1,3-diphenylurea	**4.28**	**0.01**	**0.03**	
13	1-Cl-indolocarbazole	**4.24**	**0.01**	**0.03**	
27	(4-CF_3-phenyl)thiourea	**4.23**	**0.01**	**0.03**	
28	N-(2,4,6-triclorophenyl)thiourea	**4.13**	**0.02**	**0.04**	
19	1-(4-$MeOOCC_6H_4$)-3-hexylthiourea	**4.09**	**0.01**	**0.03**	
20	1-(4-I-phenyl)-3-hexylthiourea	**3.87**	**0.01**	**0.03**	
12	**1,10-Cl_2-indolocarbazole**	**3.84**	**0.01**	**0.03**	
11	1,10-$(CF_3)_2$-indolocarbazole	**3.36**	**0.05**	**0.06**	

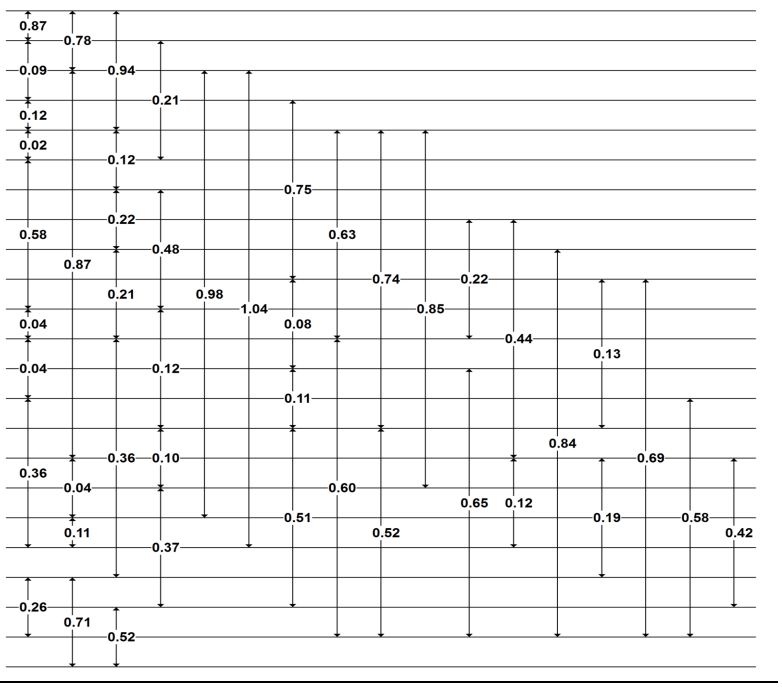

[a] Solvent: acetonitrile with 0.5% water (m/m). 1:1 stoichiometry was confirmed in all cases. Absolute logK_{ass} values are found by anchoring the scale to the logK_{ass} of compounds indicated in bold. [b] Standard uncertainties for comparing logK_{ass} values on the scale. [c] Standard uncertainties for comparing logK_{ass} values with those from other research groups.

^{1}H NMR based relative binding affinity measurement

NMR measurement observes the competitive binding between receptor molecules towards selected anion in the mixture. Protons that participate in HB exhibit change in their chemical environment and thus the extent of their shielding changes. Under the fast exchange conditions, the chemical shifts of the proton involved in HB of the free and complexed receptor are averaged and in the spectrum we see the average of the two signals instead of separate signals. As the hydrogen bond is formed the proton is deshielded and its chemical shift (δ) becomes higher. Because binding interaction of each receptor can be followed directly from the titration of the mixture of receptors with the anion, the degrees of association can be found directly from the change in chemical shifts of the protons corresponding to the receptor molecules. In current context proton signals that were observed were NH protons that behaved as HBD in the interaction with acetate anion. The degrees of association are calculated by presuming that each receptor in the mixture has reached fully complexed state. This puts a boundary on the difference in binding affinity that can be measured. If one receptor has significantly higher affinity towards selected anion, then it will be almost fully in complex before other receptors start to bind. It was found that $\Delta\log K_{ass}$ values up to 1.5 unit could be measured with reasonable accuracy.

While it is possible to measure several receptors in a single mixture, peak overlap and merging can cause challenges in identifying the right peaks of each receptor. Receptors having mutliple different NH groups can over-crowd the spectrum and increase possibilities for peak overlap. Massive dilution of the solution can cause peak broadening and disappearance. Care should be taken when choosing the concentration range for the titration experiment. DMSO was used instead of acetonitrile as solvent medium for development of NMR based $\Delta\log K_{ass}$ measurement method. More recently synthesized compounds had challenges in dissolving in acetonitrile.

As NMR based $\Delta\log K_{ass}$ measurement method was a further development of the UV-vis spectrophotometric method it was necessary to confirm that the two give comparable results. Binding studies towards acetate anion with both NMR and UV-vis method were performed. The results indicated that there was no significant difference in the obtained values. The relative binding affinity scale of acetate in DMSO is given in Table 4.

Table 4. Relative binding scale of acetate in DMSO (d_6):H_2O (99.5% : 0.5% m/m) .[a]

No	Receptor molecule	logK_{ass}	u_c[b]	u_c[c]	ΔlogK_{ass}
35	3,4,4-Cl_3-diphenylurea	4.01	0.01	0.05	
11	1-(3-NO_2-phenyl)-3-phenylurea	3.78	0.01	0.05	
30	4-NO_2-indolocarbazole	3.76	0.01	0.05	
29	4,7-Cl_2-indolocarbazole	3.72	0.01	0.05	
1	2,9-$(BuOCO)_2$-indolocarbazole	3.70	0.01	0.05	
2	2,7-$(BuOCO)_2$-indolocarbazole	3.67	0.01	0.04	
3	4,7-$(BuOCO)_2$-indolocarbazole	3.65	0.01	0.05	
9	O-Phenylenediaminourea	3.58	0.01	0.05	
31	2-NO_2-indolocarbazole	3.57	0.01	0.05	
28	2,7-Cl_2-indolocarbazole	3.55	0.01	0.05	
16	4-NO_2-C_6H_4-CH_2-OCO-indolocarbazole	3.47	0.01	0.05	
19	CH_3-CO-CH_2-OCO-Indolocarbazole	3.46	0.01	0.05	
20	2-EtO-CO-Indolocarbazole	3.46	0.01	0.05	
21	$(CH_3)_2$CH-OCO-Indolocarbazole	3.45	0.01	0.05	
17	4-MeO-C_6H_4-OCO-indolocarbazole	3.44	0.01	0.05	
18	3-CH_3-C_6H_4-CH_2-OCO-indolocarbazole	3.43	0.01	0.04	
15	Ph-CH_2-OCO-Indolocarbazole	3.43	0.01	0.04	
12	2-BuOCO-indolocarbazole	3.42	0.01	0.05	
27	2,9-Cl_2-indolocarbazole	3.40	0.01	0.05	
13	4-BuOCO-indolocarbazole	3.39	0.01	0.04	
36	1,3-diphenylurea	3.20	0.01	0.04	
5	4,7-$(CH_3)_2$-indolocarbazole	3.17	0.01	0.05	
33	2-MeO-indolocarbazole	3.15	0.01	0.05	
32	4-MeO-indolocarbazole	3.14	0.01	0.05	
24	2,7-$(MeO)_2$-indolocarbazole	3.14	0.01	0.04	
23	2,9-$(MeO)_2$-indolocarbazole	3.14	0.01	0.05	
22	Indolocarbazole	3.14	0.01	0.05	
4	2,9-$(CH_3)_2$-indolocarbazole	3.11	0.01	0.04	
34	1-Cl-indolocarbazole	2.76	0.01	0.05	
10	1-Naphthalen-1-yl-3-phenyl-urea	2.72	0.03	0.05	
8	1-CF_3-indolocarbazole	2.50	0.01	0.04	
26	1,10-Cl_2-indolocarbazole	2.15	0.01	0.04	
25	1,10-$(CF_3)_2$-indolocarbazole	1.69	0.02	0.05	

[a] Solvent: DMSO-d_6 with 0.5% water (m/m), in all cases 1:1 stoichiometry. ΔlogK_{ass} values in rectangles were determined by using the UV-Vis method.[b] Standard uncertainties for comparing logK_{ass} values on the scale. [c] Standard uncertainties for comparing logK_{ass} values with those from other research groups

4.2. Experimental study of HBD compounds

In conjunction with computational studies presented in publication V an experimental study was performed to further elucidate the hydrogen bond donor properties of a set of compounds. In total 21 neutral HBD compounds were studied via NMR based relative binding affinity measurement with chloride, chosen as the standard HBA (see Table 5). The selection of HBD was comprised of (thio)ureas, N-heterocycles, phenols and fluorinated alcohols.

Measurements of binding constants with chloride anion were performed between 2 or 3 HBD compounds. Example of ^{1}H NMR titration experiment with chloride is presented in Figure 4. N,N'-diphenylurea, indolocarbazole, 4-NO_2-indolocarbazole, thiourea and urea are bidentate HBD-s. All other compounds were monodentate HBD-s. In the selection of compounds HBD group acidity was important. Too high acidity caused broadening and disappearance of proton signals during chloride addition, because of acceleration of proton exchange.

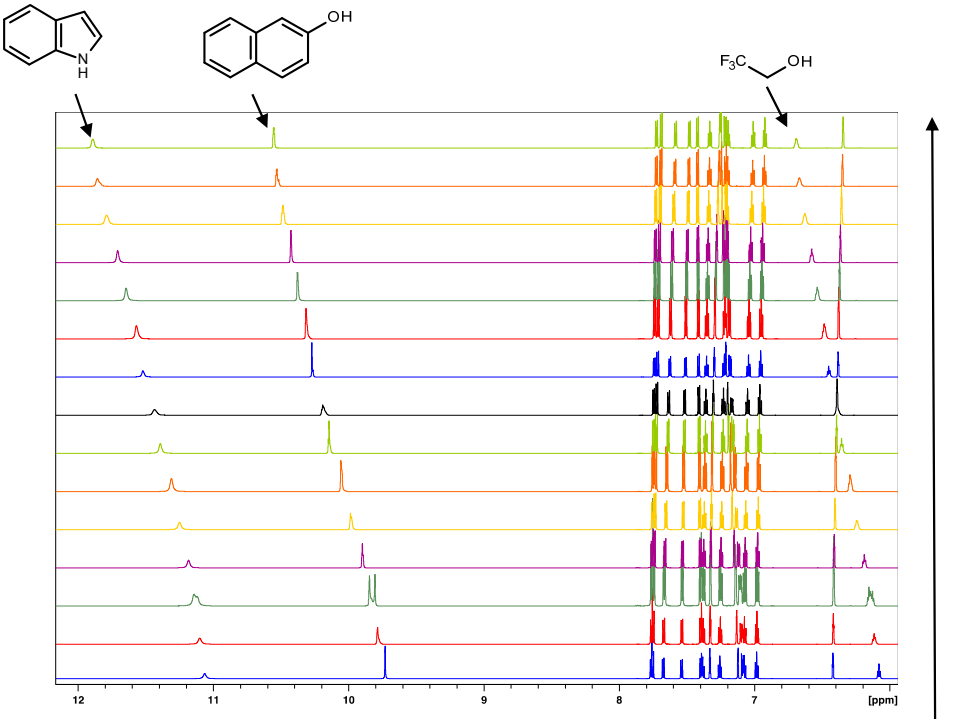

Figure 4. Indole, 2-naphtol, 2,2,2-trifluoroethanol mixture titration with TBACl in DMSO-d_6:H_2O (99.5%:0.5% m/m) at 25 °C. The titration proceeds from bottom to top.

Table 5. Relative binding scale of chloride in DMSO (d_6):H_2O (99.5% : 0.5% m/m).

Rank	HB donor	logK_{ass}	u_c [a]	u_c [b]	ΔlogK_{ass}
1	N,N'-Diphenylurea	1.52	0.02	0.07	
2	4-Nitroindolocarbazole	1.46	0.01	0.07	
3	Indolocarbazole	1.34	0.02	0.07	
4	3-Nitrophenol	0.85	0.03	0.07	
5	Thiourea	0.82	0.02	0.07	
6	3-Fluorophenol	0.76	0.03	0.07	
7	4-Bromophenol	0.71	0.01	0.07	
8	2-Naphthol	0.63	0.03	0.07	
9	$(CF_3)_2CHOH$	0.63	0.04	0.08	
10	Phenol	0.62	0.03	0.07	
11	Imidazole	0.59	0.02	0.07	
12	1-Naphthol	0.59	0.01	0.07	
13	Urea	0.55	0.03	0.07	
14	Indazole	0.54	0.03	0.07	
15	Benzimidazole	0.52	0.03	0.07	
16	4-Nitroaniline	0.52	0.02	0.07	
17	2-Methylimidazole	0.46	0.03	0.07	
18	Carbazole	0.44	0.02	0.07	
19	$(CF_3)_2CH_3COH$	0.42	0.01	0.07	
20	CF_3CH_2OH	0.41	0.01	0.07	
21	Indole	0.30	0.02	0.07	

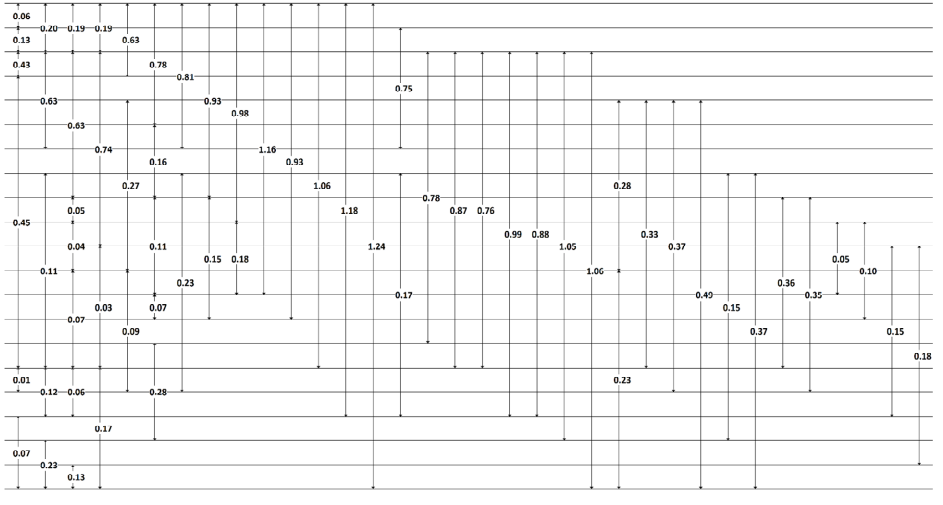

[a] Standard uncertainties for comparing logK_{ass} values on the scale. [b] Standard uncertainties for comparing logK_{ass} values with those from other research groups

4.3. Absolute binding constant measurements of glyphosate binding receptors

Molecules for binding the glyphosate dianion (Gly^{2-}) were based on indolocarbazole, urea and carbazole fragments (see Scheme 4).

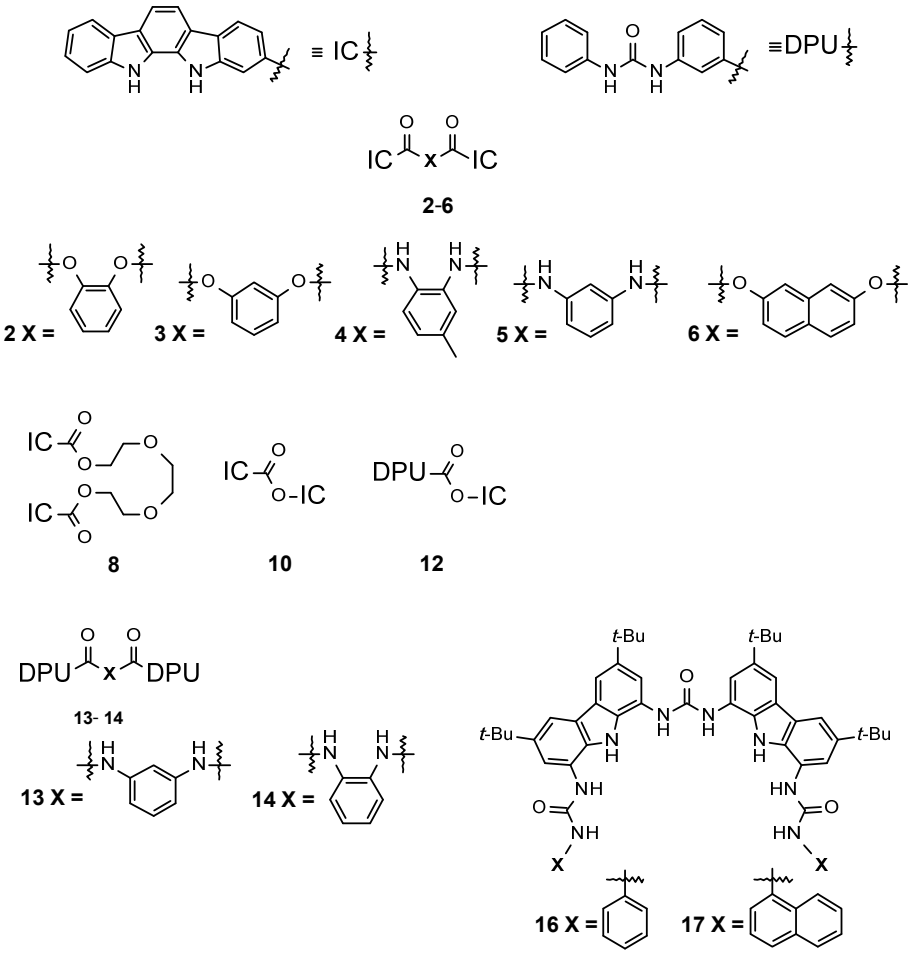

Scheme 4. Molecular structures of glyphosate receptors.

Binding constants ($\log K_{ass}$) of receptors **2**–**6**, **8**, **10**, **12**–**14** and **16**–**17** with Gly^{2-} were determined using absolute UV-vis and fluorescence titration methods (see Table 6). Large differences in binding affinity between receptors towards Gly^{2-} accompanied with high spectral overlap made UV-vis based relative binding affinity measurements difficult. Strong broadening of NH proton signals in ^{1}H NMR during TBA Gly^{2-} addition did not enable to accurately measure binding constants with NMR. For **17** $\log K_{ass}$ value in 0.5% H_2O:DMSO could

not be measured due to limitations in concentration (very high binding affinity necessitated using very low concentrations) and poor fluorescence emission.

Table 6. Binding affinity of receptors **2**–**17** for glyphosate in DMSO (0.5, 5, 10, 20 H_2O % m/m)[a]

Receptor	0.5% H_2O	5% H_2O	10% H_2O	20 % H_2O	$\Delta\log K_{ass}$ in rising H_2O content		
	$\log K_{ass}$	$\log K_{ass}$	$\log K_{ass}$	$\log K_{ass}$	0.5-5.0%	5-10%	10-20%
2	5.1	4.4	4.0	3.4	0.7	0.4	0.6
3	4.1	3.6	2.9	*d*	0.6	0.7	*e*
4	5.9[b]	5.0[b]	4.1	*d*	1.0	0.9	*e*
5	4.6	4.1	3.5	*d*	0.4	0.6	*e*
6	3.6	3.3	2.7	*d*	0.3	0.5	*e*
8	4.7	3.9	3.3	*d*	0.9	0.6	*e*
10	3.9	3.2	<2	*d*	0.7	*e*	*e*
12	4.0	3.0	<2	*d*	1.0	*e*	*e*
13	4.0	3.7	3.0	*d*	0.3	0.8	*e*
14	4.0	3.9	3.2	2.3	0.1	0.7	1.0
16	4.8[b]	3[b]	3[b]	*d*	1.7	0.0	*e*
17	*c*	6.5[b]	5.5[b]	*d*	*e*	0.9	*e*

[a] Gly^{2-} was used in the form of tetrabutylammonium (TBA) salt. [b] $\log K_{ass}$ values with these receptors measured via fluorescence, with the remaining receptors UV–Vis method was used. Receptor **4** was measured using both techniques, see the Experimental section. [c] Binding constant was too high for measurement. [d] Receptor insoluble in 20% H_2O:DMSO mixture. [e] $\Delta\log K_{ass}$ between the respective H_2O:DMSO mixtures could not be calculated.

5. DISCUSSION

5.1. Characteristics of relative binding affinity measurements

Advantages and disadvantages of UV-vis- and NMR-based relative binding affinity techniques are outlined in Table 7.

Table 7. Comparison of UV-vis and NMR based relative binding affinity methods

Method	UV-vis	NMR
Advantages	• Instrument's high sensitivity enables working with lower concentrations. • Easier instrument operation. • Significantly lower cost of purchase and maintenance.	• Spectra give much more information. • Simpler data treatment method. • Spectral overlap is infrequent. • Possible to measure several $\Delta\log K_{ass}$ values in single run.
Disadvantages	• Very serious spectral overlap. • Complex calculation method. • Time consuming measurement. • Necessary to titrate single receptor before mixture.	• Instrument's low sensitivity. • In most cases deuterated solvents are needed. • High purchase and maintenance costs. • Fast moving protons can broaden during titration and decrease chemical shift determination accuracy.

To conclude comparison of the two above discussed methods, the availability of NMR instrument can help to decrease measurement time, improve accuracy and simplify the calculation method for relative binding constant measurement. However, one should take into account the much larger amounts of compounds needed for measurements, potential signal broadenings and peak overlaps. UV-vis spectrophotometric method is far more time consuming and requires significantly more complex calculation procedure. Also, heavy spectral overlap is more frequent and more care should be taken when choosing receptor pairs. At the same time, very small quantities of compounds are sufficient for the UV-Vis method.

5.2. Carboxylate discrimination studies through relative binding affinities

Relative binding affinity measurement is very useful to compare the binding strength of two receptors towards a single anion. Also, it can be employed to examine the cross-selective properties of the receptors.

Acetate, trimethylacetate, lactate and benzoate were included in the study as small anionic species (further discussed in publication IV). These are among the simplest carboxylate anions. And studying their binding gives more insight into carboxylate binding characteristics. Acetate has smallest steric effects (besides formate) and is one of the most hydrophilic carboxylates. In contrast, trimethylacetate and benzoate are hydrophobic, but differ by the nature of the hydrocarbon residue (aromatic vs aliphatic). Lactate has hydroxyl group that can form additional HBs with the receptor and is the least basic of the four. Such selection gives as much diversity in anion basicity, hydrophobicity/hydrophilicity and steric effects, as is possible with small number of anions. It became very clear that basicity of the anion dominated in selectivity. It is easy to agree with the statement that designing selective receptor for highly basic anion is easier than for weakly basic one. Higher basicity is often associated with higher HBA and charge density. Higher negative charge density will draw more strongly the partial positive charges of the HB donor binding moieties of the receptor molecule.

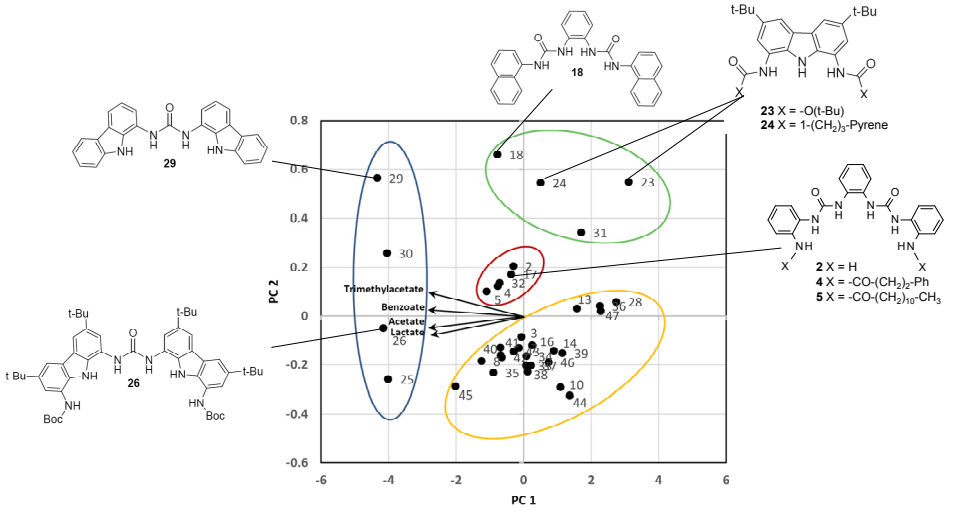

Figure 5. PCA plot of binding constant data: Scores of PC2 vs scores of PC1.

PCA was performed on the binding constant data to further assess the differences between the selectivity patterns of the receptors involved in this study, i.e. the possibility of finding receptors able to differentiate between the targeted carboxylate ions. This kind of multivariate analysis of data from a number of receptors is the basis of achieving selectivity by receptor arrays, where none of

the individual receptors by themselves are selective enough.[37] The plot of scores of different receptors according to the PC1 and PC2 is presented in Figure 5. PC1 describes 97% of the variance. The axes of binding constants of all four anions are quite well aligned with PC1, so PC1 shows the general binding affinity of the receptors towards the carboxylate anions. The receptors having highest binding affinities are positioned to the left hand side of the plot. PC2 describes 2% of the variance. Looking at the axes of the binding constants of the anions indicates that PC2 characterizes the selectivity between large hydrophobic and small hydrophilic ions. Receptors that have (relatively) lower affinity towards acetate and lactate and relatively higher affinity towards trimethylacetate and benzoate are positioned in the upper part of the plot. Strong difference in binding is evident between acetate and trimethylacetate to receptor **29**. Examination of the geometries of the anion-receptor complexes shows that the "binding pocket" of **29** exactly accommodates pivalate enabling some solvophobic interaction between its *t*-Bu group and the outer aromatic rings of the carbazole fragments. For acetate the pocket is too big and no similar interactions with the aromatic rings is possible. The plot also reveals that the selectivity patterns of the used receptors towards acetate and lactate are very similar (although absolute binding affinities differ). Four groups of receptors emerge on the plot: (1) Receptors **25**, **26**, **29** and **30**, which are the strongest binders; (2) Receptors **18**, **23, 24** and **31**, which have relatively the strongest affinity towards trimethylacetae, supposedly made possible by hydrophobic/ solvophobic interaction; (3) Receptors **2, 4, 5, 17** and **32**, which are all based on combining two ureas via an 1,2-phenylene fragment and can also possibly have some solvophobic interaction and (4) all other receptors, which seem to bind anions mostly by hydrogen bonding, without significant involvement of other interactions. Examining the PCA plot together with the structural features can be of help in picking molecular fragments for designing new receptors.

5.3. Characteristics of glyphosate binding receptors

Glyphosate has significantly more complex structure than most of the anions for which receptor molecules are designed. Gly^{2-} possesses 3 basic centers: phosphonate ($R\text{-}PO_3H^-$), carboxylate ($R\text{-}COO^-$) and amine (R-NH-R). Their pK_a values (corresponding to protonation of these sites) in aqueous media are pK_{a2} = 2.09, pK_{a3} = 5.52 and pK_{a4} = 10.28, respectively.[88] In this work these pK_a values can be used only as approximate guides, because binding of Gly^{2-} is studied in DMSO-water mixtures, not in pure water, and protonation behavior of Gly^{2-} is also affected by the receptors' HBD and HBA groups. We will present below some evidence that this is indeed the case in some complexes between Gly^{2-} and anion receptors. The anionic COO^- and PO_3H^- moieties of Gly^{2-} are facing the opposite directions. Thus, if a receptor is to form hydrogen bond (HB) with both of them, the receptor must be big enough, i.e. the hydrogen bond donor (HBD) groups must be linked by a spacer that is long

enough, as is well illustrated by computational geometries in Figure 6 a, c, h. The positions and charge distribution on the anionic centres of Gly^{2-} are further modulated by the NH fragment. It has weak intramolecular HB interaction (distance 1.90 Å) with the OH of the PO_3H^- (Figure 6, Gly^{2-}). The NH also interacts to some extent with one of the COO^- oxygen atoms (distance 2.39 Å). The remaining two oxygen atoms of PO_3H^- are strong HB acceptors and are responsible for HBs in most of the complexes (Figure 6 a, c, h). According to computations, in cases when the receptor geometry favors binding of all three O atoms of PO_3H^- (receptors **4**, **14**, **16**, **17**) the H^+ tautomerizes from phosphonate to the –NH– group forming $–NH_2^+–$. Interactions with the $–NH_2^+–$ fix the anionic groups in Gly^{2-} with respect to each other in such a way that the four oxygen atoms are not far from being in the same plane. Furthermore, the carboxylate group forms appreciable intramolecular HB with $–NH_2^+–$. Therefore, as an overall effect, the HB acceptor ability of the phosphonate end increases and that of COO^- decreases. This can lead to binding of Gly^{2-} by the phosphonate end only.

Glyphosate binding receptors **2**–**6**, **8** and **10** featuring IC HBD fragments linked at position 2 were prepared to study spacer effects on binding. IC fragments were chosen, because they are more rigid and their HBD donor NH groups are spatially fixed in one direction. Spacer can differ by their chemical nature, length, rigidity and polarity. This introduces substantial workload for testing large variety of potential spacers. Receptors **2**–**6** have aromatic spacers which are less flexible while receptor **8** has a very flexible spacer. Both spacer flexibility and length can affect binding quite strongly. As glyphosate has rather rigid structure the receptor has to have either suitable pre-orientation or be able to change its geometry to bind glyphosate. Receptors **2**, **3** and **6** share ester linkage and comparable spacer rigidity, however, differ by spacer length (increasing from **2** to **6**) and angular positions of the binding moieties. A reasonable initial assumption was that longer and more rigid naphthalene spacer of **6** would result in stronger binding of Gly^{2-}. Experimental findings proved the opposite with binding decreasing in the following row **2**, **3**, **6**. Receptor **6** is ~ 1.5 log units (0.5% H_2O:DMSO), ~ 1.1 log units (5% H_2O:DMSO) and ~ 1.1 log units (10% H_2O:DMSO) weaker Gly^{2-} binder than receptor **2**. Receptor **10** demonstrates that too short spacer is also not suitable. Short ester bond linkage between 2 IC fragments offer limited possibility to adjust geometry to Gly^{2-}. As stated above, receptor **8** was designed to have an extremely flexible spacer. It serves as a reference that can orient IC fragments in almost any geometry to bind Gly^{2-} with small steric strain in the complex (see Figure 6 h). It gives information about the most preferred orientations of binding moieties from the computational geometries in the case of two bidentate binding moieties forming tetradentate complex with Gly^{2-} anion. Although, there is only negligible strain in the complex, Gly^{2-} binding to **8** ranks in the middle of the group. This is most probably due to significant penalty in entropy, because of considerable decrease in the number of conformations of free **8** to the few favourable conformations of the Gly^{2-} complex upon binding.

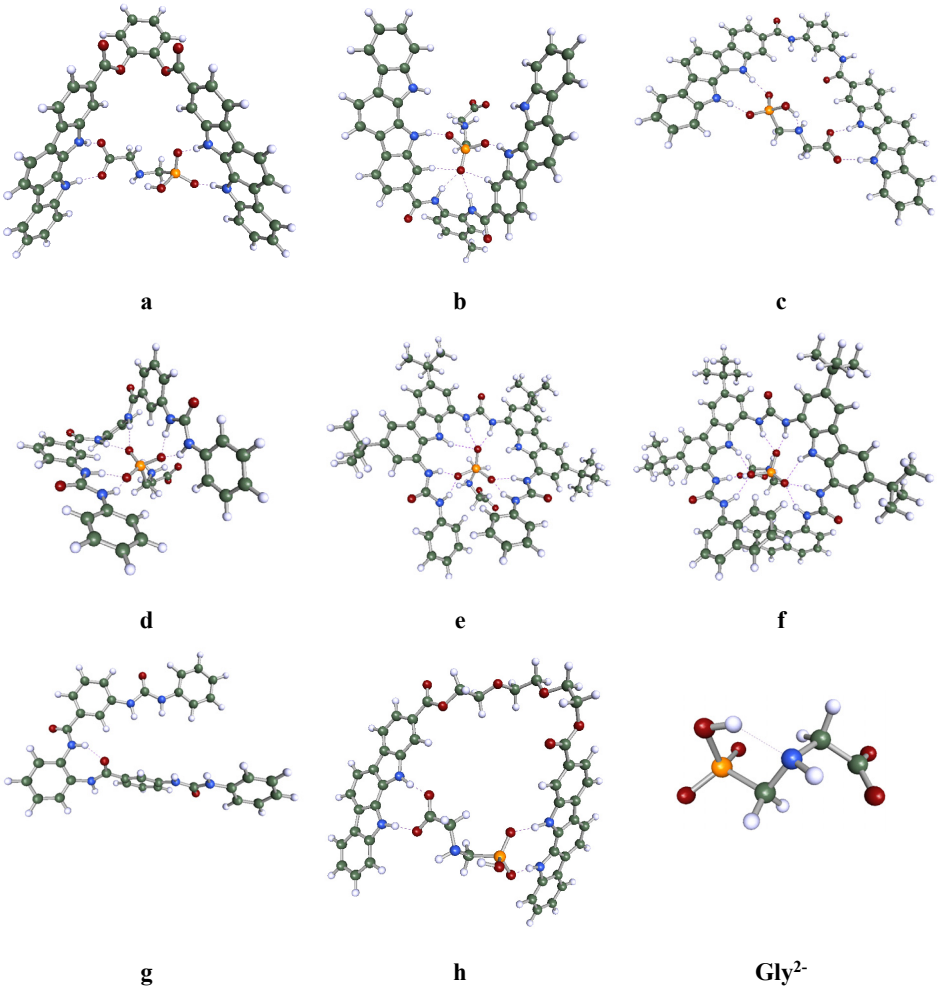

Figure 6. Computational (COSMO-RS, see the SI) geometries of receptor-Gly^{2-} complexes a) Receptor (2) + Gly^{2-}. b) Receptor (4) + Gly^{2-}. c) Receptor (5) + Gly^{2-}. d) Receptor (14) + Gly^{2-}. e) Receptor (16) + Gly^{2-}. f) Receptor (17) + Gly^{2-}. g) Free receptor 14. h) Receptor 8 + Gly^{2-}.

In general, 1,2-disubstituted aromatic rings having more suitable angular position enable to bind Gly^{2-} with higher affinity than 1,3-disubstituted rings. Switching substitution positions in the spacer from 1,3 to 1,2 in such receptors increases Gly^{2-} binding affinity by around 1 log unit (in 0.5% H_2O:DMSO) in receptor pairs **4** vs **5** and **2** vs **3**. In fact **4** has higher affinity towards Gly^{2-} than any of the remaining receptors except **17**. Comparison of **4** to **2** and **5** to **3** enables to compare amide to ester linkage. It showed that amide linkers enable higher Gly^{2-} affinity. Rigid and fixed spacer with optimal length and spatial orientation seemed the most reasonable choice so that the receptor could assume the most suitable geometry for complexation with glyphosate. Therefore, benzene- or

naphthalene-based aromatic spacers were selected for achieving more fixed and suitably preoriented receptor structure. The results show that such spacers do not necessarily lead to high binding affinity as demonstrated by the naphthalene spacer of **6** – although by its length and spatial orientation of the binding moieties it seemed very suitable, **6** is the weakest Gly^{2-} binder out of all compounds investigated. The weakness of binding Gly^{2-} by **6** indirectly confirms the hypothesis that Gly^{2-} is bound to receptors first of all by the phosphonate end. Among the IC-based compounds the binding affinity in 0.5% H_2O:DMSO towards Gly^{2-} decreases in the order **4** > **2** > **8** > **5** > **3** > **10** > **6**.

Although, similar by their acidity in DMSO and by the placement and orientation of the NH groups, diphenylurea and IC have different binding properties of respective receptors with Gly^{2-}. IC-based receptors **4** and **5** differ from each other by 1.3 $\log K_{ass}$ units in DMSO with 0.5% of H_2O. In contrast, urea-based receptors **13** and **14** with nearly identical spacers differ in the same solvent mixture by less than 0.05 $\log K_{ass}$ units.

Influence on water content was studied in 4 DMSO:H_2O mixtures. Because receptors are solvated differently in water rise in water content in DMSO shows different sensitivity to binding affinity. In example, at low water content (0.5% H_2O) **4** has by 0.8 log units higher affinity than **2**. In a more aqueous solvent the amide fragments in **4** form HBs more readily with solvent molecules. As a result, in DMSO with 10% of water **2** and **4** have almost equal affinity towards Gly^{2-}. **4** and **14** have identical spacers and differ by the binding moieties (IC vs DPU). This causes the binding affinity to differ by around 2 log units in DMSO with 0.5% of water. Increasing the water content to 10% decreases this difference to around 1 log unit. According to computations the amide NH proton in the spacer of free **14** can form HB with another amide group, which is disrupted on binding to Gly^{2-}. Water-rich solvent suppresses this intramolecular HB and thus favors removing this "obstacle" to binding Gly^{2-}.

Elucidation of experimental and computational results suggests that glyphosate may primarily be bound by the phosphonate group only. This is evidenced by receptors **4**, **14**, **16** and **17**, which are shown to bind by phosphonate. Interaction of receptor **17** with Gly^{2-} was further investigated with NMR. ^{1}H NMR titration shows that all NH protons of urea, amide and carbazole experience deshielding, which suggests the involvement of those protons in hydrogen bonding. This is further supported by 2D NMR experiments.

SUMMARY

The thesis focuses on the development of relative equilibrium constant measurement methods and studying their applicability in different fundamental studies related to acid-base equilibria and anion binding by molecular receptors. UV-vis spectrophotometric relative equilibrium constant measurement was used to characterize basicity of phosphanes and diphosphanes and binding of acetate anion towards synthetic receptors. For a set of different bases 21 pK_a values were determined in acetonitrile. Additionally, 23 logK_{ass} values for 23 different synthetic receptors towards acetate in acetonitrile with 0.5% water were determined. As a further development, the relative measurement method was implemented using ^{1}H NMR. The latter has much better intrinsic selectivity and thereby allows measuring several binding constants in a single run. The main downside for NMR is its low sensitivity which requires more compound for experiments. NMR based relative binding affinity technique was validated by set of measurements performed with UV-vis spectrophotometry. Both measurement techniques showed good agreement with each other. The same NMR based method was applied to study HBD properties of a set of 21 HBD compounds towards chloride in DMSO-d_6:H_2O (99.5% : 0.5% m/m).

Subsequent study of binding small carboxylate anions (acetate, trimethylacetate, benzoate, lactate) with different molecular receptors was performed, mainly on NMR. In interactions where hydrogen bonding is the main contributor anion basicity becomes the dominating factor to influence binding sensitivity and selectivity. Principal component analysis of measured binding constants shows strong dependence of binding on the number of NH groups, their spatial position and HBD properties.

Binding glyphosate dianion – an important herbicide and target analyte for supramolecular analytical applications – was studied separately from other discussed anions in DMSO (0.5, 5, 10, 20 H_2O % m/m). The influence of water content varies between urea, carbazole and indolocarbazole receptors and is not straightforward. Also, it is well demonstrated how small deviations in receptor structure can have large influence on its binding abilities. Thus, predicting binding affinity of a molecular receptor by some general structural features is not possible and accurate experimental study is critical to assess its sensitivity and selectivity.

The results presented in work are helpful in further development of supramolecular structures for binding of various anionic substrates (analytes) by assessing their acid-base, HBD and binding properties.

SUMMARY IN ESTONIAN

Kvantitatiivsed suhtelise tasakaalu konstandi määramise meetodid supramolekulaarses keemias

Käesoleva töö peamiseks fookuseks oli suhteliste tasakaalukonstandi mõõtmismeetodite arendamine ja rakendatavuse uurimine erinevate fundamentaalsete vastasmõjude uurimisel. UV-vis spektrofotomeetrilist suhtelist tasakaalukonstantide mõõtmise meetodit rakendati selleks, et uurida fosfaanide ja difosfaanide aluselisust ning atsetaadi seondumist sünteetiliste retseptor molekulide külge. Aluselisuse iseloomustamiseks atsetonitriilis määrati 21 pK_a väärtust. Lisaks määrati 23 logK_{ass} väärtust atsetaadi ja 23 sünteetilise retseptori suhtes 0,5% veesisaldusega atsetonitriilis. UV-vis spektrofotomeetrilise seondumisafiinsuse määramise meetodi edasi arendus on TMR baasil versioon, mis võimaldab mõõta mitu seondumiskonstanti ühe mõõtmisega. Puuduseks on TMR madalam tundlikkus, mille tõttu on vajalik suurem kogus ainet. TMR põhist suhtelise seondumisafiinsusmõõtmise meetodit valideeriti UV-vis spektrofotomeetriaga. Mõlemad mõõtemeetodid näitasid head kooskõla. Sama TMR põhist meetodid rakendati ka 21 ühendi vesiniksideme donoorsuse uurimiseks kloriidi suhtes DMSO-d_6:H_2O (99.5% : 0.5% m/m) keskkonnas.

Atsetaat aniooni seondumisele järgnev uurimus kaasas trimetüülatsetaadi, bensoaadi ja laktaadi. Vastasmõjudes, kus vesinikside on peamiseks mõjuriks, muutub aniooni aluselisus üheks peamiseks seondumise tundlikkust ja selektiivust mõjutavaks faktoriks. Määratud seondumiskonstantide põhjal tehtud peakomponentide analüüs näitas lisaks ka seondumis tugevat mõju retseptori NH rühmade arvu, ruumilise paigutuse ja vesiniksideme donoorsuse vahel.

Glüfosaadi, olulise herbitsiidi ja supramolekulaarsete analüütiliste rakenduste analüüdi, seondumist uuriti teistest töös käsitletud karboksülaatidest eraldi. Mõõdeti logK_{ass} väärtused 12 sünteetilisele retseptorile glüfosaadi suhtes DMSO (0.5, 5, 10, 20 H_2O % m/m) segudes. Veesisalduse mõju tugevus varieerub uurea, karbasooli ja indolokarbasooli tüüpi retseptorite vahel. Väikesed muutused retseptori struktuuris põhjustavad märkimisväärseid muutusi seondumisafiinsuses. Tundlikkuse ja selektiivsuse hindamiseks on oluline täpsed eksperimentaalsed uuringud.

Käesolevas töös esitatud tulemused on olulised edasiste supramolekulaarsete ühendite väljatöötamisel, hinnates nende happelis-aluselisi, vesiniksideme donoorseid ja seondumise omadusi.

REFERENCES

[1] J.-M. Lehn, *Angew. Chem. Int. Ed. Engl.* **1988**, *27*, 89–112.
[2] J.-M. Lehn, *Angew. Chem. Int. Ed.* **2013**, *52*, 2836–2850.
[3] J. W. Steed, J. L. Atwood, *Supramolecular Chemistry*, John Wiley And Sons, Ltd, Chichester, **2009**.
[4] B. Dietrich, J. M. Lehn, J. P. Sauvage, *Tetrahedron Lett.* **1969**, *10*, 2889–2892.
[5] D. J. Cram, J. M. Cram, *Science* **1974**, *183*, 803–809.
[6] C. J. Pedersen, *J. Am. Chem. Soc.* **1967**, *89*, 7017–7036.
[7] V. Balzani, M. Gómez-López, J. F. Stoddart, *Acc. Chem. Res.* **1998**, *31*, 405–414.
[8] J. W. Pflugrath, F. A. Quiocho, *Nature* **1985**, *314*, 257–260.
[9] J.-M. Lehn, *Science* **1985**, *227*, 849–856.
[10] C. Schmuck, *Nat. Nanotechnol.* **2011**, *6*, 136–137.
[11] T. Rehm, C. Schmuck, *Chem. Commun.* **2008**, *0*, 801–813.
[12] J. M. Lehn, *Science* **2002**, *295*, 2400–2403.
[13] E. V. Anslyn, D. A. Dougherty, *Modern Physical Organic Chemistry*, University Science Books, Sausalito (Calif.), **2006**.
[14] P. D. Beer, P. A. Gale, *Angew. Chem. Int. Ed.* **2001**, *40*, 486–516.
[15] N. H. Evans, P. D. Beer, *Angew. Chem. Int. Ed.* **2014**, *53*, 11716–11754.
[16] K. Bowman-James, A. Bianchi, E. García-España, Eds. , *Anion Coordination Chemistry*, Wiley-VCH, Weinheim, **2012**.
[17] S. Mangani, M. Ferraroni, in *Supramol. Chem. Anions* (Eds.: A. Bianchi, K. Bowman-James, E. Garcia-España), Wiley, New York, **1997**, pp. 63–78.
[18] C. H. Park, H. E. Simmons, *J. Am. Chem. Soc.* **1968**, *90*, 2431–2432.
[19] E. Graf, J. M. Lehn, *J. Am. Chem. Soc.* **1976**, *98*, 6403–6405.
[20] J. M. Lehn, E. Sonveaux, A. K. Willard, *J. Am. Chem. Soc.* **1978**, *100*, 4914–4916.
[21] F. P. Schmidtchen, G. Müller, *J. Chem. Soc., Chem. Commun.* **1984**, 1115–1116.
[22] E. Fan, A. Scott, V. Arman, S. Kincaid, A. D. Hamilton, *J. Am. Chem. Soc.* **1993**, *115*, 369–370.
[23] M. D. Best, S. L. Tobey, E. V. Anslyn, *Coord. Chem. Rev.* **2003**, *240*, 3–15.
[24] S. L. Tobey, B. D. Jones, E. V. Anslyn, *J. Am. Chem. Soc.* **2003**, *125*, 4026–4027.
[25] J. L. Sessler, M. J. Cyr, V. Lynch, E. McGhee, J. A. Ibers, *J. Am. Chem. Soc.* **1990**, *112*, 2810–2813.
[26] A. E. Hargrove, S. Nieto, T. Zhang, J. L. Sessler, E. V. Anslyn, *Chem. Rev.* **2011**, *111*, 6603–6782.
[27] E. V. Anslyn, *J. Org. Chem.* **2007**, *72*, 687–699.
[28] M. Más-Montoya, M. Cuartero, D. Curiel, J. A. Ortuño, M. Soledad García, A. Tárraga, *The Analyst* **2015**, *140*, 287–294.
[29] O. S. Wolfbeis, *Angew. Chem. Int. Ed.* **2013**, *52*, 9864–9865.
[30] P. Anzenbacher, Jr., P. Lubal, P. Buček, M. A. Palacios, M. E. Kozelkova, *Chem. Soc. Rev.* **2010**, *39*, 3954.
[31] M. Wenzel, J. R. Hiscock, P. A. Gale, *Chem Soc Rev* **2012**, *41*, 480–520.
[32] C. J. E. Haynes, S. N. Berry, J. Garric, J. Herniman, J. R. Hiscock, I. L. Kirby, M. E. Light, G. Perkes, P. A. Gale, *Chem Commun* **2013**, *49*, 246–248.
[33] P. Piątek, *Chem. Commun.* **2011**, *47*, 4745.

[34] M. Orłowska, M. Mroczkiewicz, K. Guzow, R. Ostaszewski, A. M. Kłonkowski, *Tetrahedron* **2010**, *66*, 2486–2491.
[35] M. A. Yawer, V. Havel, V. Sindelar, *Angew. Chem. Int. Ed.* **2015**, *54*, 276–279.
[36] Y. Miyahara, K. Goto, M. Oka, T. Inazu, *Angew. Chem. Int. Ed.* **2004**, *43*, 5019–5022.
[37] J. J. Lavigne, E. V. Anslyn, *Angew. Chem. Int. Ed.* **2001**, *40*, 3118–3130.
[38] H.-J. Schneider, *Angew. Chem. Int. Ed.* **2009**, *48*, 3924–3977.
[39] F. Biedermann, H.-J. Schneider, *Chem. Rev.* **2016**, *116*, 5216–5300.
[40] T. Steiner, *Angew. Chem. Int. Ed.* **2002**, *41*, 48–76.
[41] E. Arunan, G. R. Desiraju, R. A. Klein, J. Sadlej, S. Scheiner, I. Alkorta, D. C. Clary, R. H. Crabtree, J. J. Dannenberg, P. Hobza, et al., *Pure Appl. Chem.* **2011**, *83*, 1637–1641.
[42] G. R. Desiraju, *Nature* **2001**, *412*, 397–400.
[43] C. Laurence, M. Berthelot, *Perspect. Drug Discov. Des.* **2000**, *18*, 39–60.
[44] J. W. Steed, D. R. Turner, K. J. Wallace, *Core Concepts in Supramolecular Chemistry and Nanochemistry*, John Wiley And Sons, Ltd, Chichester, England, **2007**.
[45] S. Alunni, A. Pero, G. Reichenbach, *J. Chem. Soc. Perkin Trans. 2* **1998**, 1747–1750.
[46] C. A. Hunter, *Philos. Trans. R. Soc. Lond. Math. Phys. Eng. Sci.* **1993**, *345*, 77–85.
[47] C. A. Hunter, K. R. Lawson, J. Perkins, C. J. Urch, *J. Chem. Soc. Perkin Trans. 2* **2001**, *0*, 651–669.
[48] J. C. Barnes, M. Juríček, N. L. Strutt, M. Frasconi, S. Sampath, M. A. Giesener, P. L. McGrier, C. J. Bruns, C. L. Stern, A. A. Sarjeant, et al., *J. Am. Chem. Soc.* **2013**, *135*, 183–192.
[49] M. Mascal, A. Armstrong, M. D. Bartberger, *J. Am. Chem. Soc.* **2002**, *124*, 6274–6276.
[50] P. de Hoog, P. Gamez, I. Mutikainen, U. Turpeinen, J. Reedijk, *Angew. Chem.* **2004**, *116*, 5939–5941.
[51] A. I. Share, A. H. Flood, *Nat. Chem.* **2010**, *2*, 349–350.
[52] C. Reichardt, T. Welton, in *Solvents Solvent Eff. Org. Chem.*, VCH, Weinheim, Germany, **2011**, pp. 7–64, 156–163.
[53] J. L. Sessler, D. E. Gross, W.-S. Cho, V. M. Lynch, F. P. Schmidtchen, G. W. Bates, M. E. Light, P. A. Gale, *J. Am. Chem. Soc.* **2006**, *128*, 12281–12288.
[54] A. Kütt, I. Leito, I. Kaljurand, L. Sooväli, V. M. Vlasov, L. M. Yagupolskii, I. A. Koppel, *J. Org. Chem.* **2006**, *71*, 2829–2838.
[55] K. Kaupmees, I. Kaljurand, I. Leito, *J. Phys. Chem. A* **2010**, *114*, 11788–11793.
[56] H. Motulsky, *Analyzing Data with GraphPad Prism*, GraphPad Software Inc., San Diego, **1999**.
[57] A. R. Katritzky, T. Tamm, Y. Wang, M. Karelson, *J. Chem. Inf. Comput. Sci.* **1999**, *39*, 692–698.
[58] J.-L. M. Abboud, R. Notario, *Pure Appl. Chem.* **1999**, *71*, 645–718.
[59] K. Hirose, in *Anal. Methods Supramol. Chem.* (Ed.: C.A. Schalley), Wiley-VCH, Weinheim, **2012**, pp. 27–66.
[60] S. Meier, S. R. Beeren, *J. Am. Chem. Soc.* **2014**, *136*, 11284–11287.
[61] J. E. Ladbury, *Biochem. Soc. Trans.* **2010**, *38*, 888–893.
[62] J. E. Ladbury, G. Klebe, E. Freire, *Nat. Rev. Drug Discov.* **2010**, *9*, 23–27.
[63] J. Tellinghuisen, *Anal. Biochem.* **2004**, *333*, 405–406.

[64] E. Freire, O. L. Mayorga, M. Straume, *Anal. Chem.* **1990**, *62*, 950A–959A.
[65] P. Dydio, D. Lichosyt, J. Jurczak, *Chem. Soc. Rev.* **2011**, *40*, 2971–2985.
[66] D. Fărcaşiu, D. Hâncu, *Catal. Lett.* **1998**, *53*, 3–6.
[67] I. L. Kirby, M. Brightwell, M. B. Pitak, C. Wilson, S. J. Coles, P. A. Gale, *Phys. Chem. Chem. Phys.* **2014**, *16*, 10943–10958.
[68] M. P. Hughes, M. Shang, B. D. Smith, *J. Org. Chem.* **1996**, *61*, 4510–4511.
[69] M. P. Hughes, B. D. Smith, *J. Org. Chem.* **1997**, *62*, 4492–4499.
[70] F. G. Bordwell, *Acc. Chem. Res.* **1988**, *21*, 456–463.
[71] V. Amendola, L. Fabbrizzi, L. Mosca, *Chem. Soc. Rev.* **2010**, *39*, 3889–3915.
[72] A.-F. Li, J.-H. Wang, F. Wang, Y.-B. Jiang, *Chem. Soc. Rev.* **2010**, *39*, 3729–3745.
[73] S.-K. Ko, S. K. Kim, A. Share, V. M. Lynch, J. Park, W. Namkung, W. Van Rossom, N. Busschaert, P. A. Gale, J. L. Sessler, et al., *Nat. Chem.* **2014**, *6*, 885–892.
[74] Y. Liu, T. Minami, R. Nishiyabu, Z. Wang, P. Anzenbacher, *J. Am. Chem. Soc.* **2013**, *135*, 7705–7712.
[75] P. A. Gale, *Chem. Commun.* **2008**, 4525–4540.
[76] D. Curiel, A. Cowley, P. D. Beer, *Chem. Commun.* **2005**, 236–238.
[77] J. Suk, K.-S. Jeong, *J. Am. Chem. Soc.* **2008**, *130*, 11868–11869.
[78] P. Vollhardt, N. Schore, *Organic Chemistry: Structure and Function*, W. H. Freeman, New York, **2011**.
[79] C. Hansch, A. Leo, D. Hoekman, *Exploring QSAR Hydrophobic, Electronic, and Steric Constants*, American Chemical Society, Washington, DC, **1995**.
[80] I. Kaljurand, A. Kütt, L. Sooväli, T. Rodima, V. Mäemets, I. Leito, I. A. Koppel, *J. Org. Chem.* **2005**, *70*, 1019–1028.
[81] L. Sooväli, I. Kaljurand, A. Kütt, I. Leito, *Anal. Chim. Acta* **2006**, *566*, 290–303.
[82] G. G. Manov, R. G. Bates, W. J. Hamer, S. F. Acree, *J. Am. Chem. Soc.* **1943**, *65*, 1765–1767.
[83] H. A. Benesi, J. H. Hildebrand, *J. Am. Chem. Soc.* **1949**, *71*, 2703–2707.
[84] V. M. S. Gil, N. C. Oliveira, *J. Chem. Educ.* **1990**, *67*, 473–478.
[85] D. B. Hibbert, P. Thordarson, *Chem. Commun.* **2016**, *52*, 12792–12805.
[86] P. Muller, *Pure Appl. Chem.* **1994**, *66*, 1077–1184.
[87] J. F. Coetzee, G. R. Padmanabhan, *J. Am. Chem. Soc.* **1965**, *87*, 5005–5010.
[88] B. C. Barja, M. dos Santos Afonso, *Environ. Sci. Technol.* **1998**, *32*, 3331–3335.

ACKNOWLEDGEMENTS

I want to express my gratitude to my supervisor Professor Ivo Leito for supervising, guiding and challenging me when needed. Carrying out given PhD project has provided me with numerous opportunities to develop my technical and interpersonal skills. It has challenged me to take on more leadership roles and guide the direction of our research in supramolecular chemistry. Learning and developing myself under Ivo's tutelage has been a great honor.

Further, I am thankful to all the members in the Chair of Analytical Chemistry for support and help. It was a tremendous pleasure to be inspired by some many proactive individuals. Mentoring my students Kerli Martin, Juuli Nõges and Indrek Saar, has made me a better student and a better teacher. Collaborative research with Sandip A. Kadam, Jaan Saame, Karl Kaupmees, Tõiv Haljasorg, Lauri Toom and Astrid Pung has given me the possibility to connect various technical experience to make great science and I am thankful for that.

Lastly, I want to thank my wife Carmen for patience and support during these years. You have been a great inspiration for me in creativity and determination. Thank you for being there to listen and support me through these challenges.

PUBLICATIONS

CURRICULUM VITAE

Name:	Kristjan Haav
Date of birth:	20.02.1989
Citizenship:	Estonian
Contact:	Institute of Chemistry, Faculty of Science and Technology, University of Tartu 14a Ravila Street, 50411 Tartu, Estonia
E-mail:	kristjanhaav@gmail.com

Education:

2005–2008	Tartu Mart Reiniku Gymnasium
2008–2011	University of Tartu – Bachelor's degree in chemistry
2011–2013	University of Tartu – Master's degree in engineering (*cum laude*)
2013–	University of Tartu – PhD student in chemistry

Professional Employment: 2012–present University of Tartu, Chemist

Scientific Publications:

1. Haav, K.; Saame, J.; Kütt, A.; Leito, I. Basicity of Phosphanes and Diphosphanes in Acetonitrile. *Eur. J. Org. Chem.*, **2012**, *11*, 2167–2172.
2. Haav, K.; Kadam, S. A.; Toom, L.; Gale, P. A.; Busschaert, N.; Wenzel, M.; Hiscock, J. R.; Kirby, I. L.; Haljasorg, T.; Lõkov, M.; Leito I. Accurate Method To Quantify Binding in Supramolecular Chemistry. *J. Org. Chem.*, **2013**, *78*, 7796–7808.
3. Kadam, S. A.; Haav, K.; Toom, L.; Haljasorg, T.; Leito, I. NMR Method for Simultaneous Host–Guest Binding Constant Measurement. *J. Org. Chem.*, **2014**, *79*, 2501–2513.
4. Kadam, S. A.; Martin, K.; Haav, K.; Toom, L.; Mayeux, C.; Pung, A.; Gale, P. A.; Hiscock, J. R.; Brooks, S. J.; Kirby, I. L.; Busschaert, N.; Leito, I. Towards the Discrimination of Carboxylates by Hydrogen-Bond Donor Anion Receptors. *Chem. Eur. J.*, **2015**, *21*, 5145–5160.
5. Tshepelevitsh, S.; Trummal, A.; Haav, K.; Martin, K.; Leito, I. Hydrogen-Bond Donicity in DMSO and Gas Phase and Its Dependence on Brønsted Acidity. *J. Phys. Chem. A*, **2017**, *121*, 357–369.
6. Kadam, S. A.; Haav, K.; Toom, L.; Pung, A.; Mayeux, C.; Leito, I. Multi-dentate anion receptors for binding glyphosate dianion: structure and affinity. *Eur. J. Org. Chem.*, **2017**, 1396–1406.
7. Liigand, P.; Kaupmees, K.; Haav, K.; Liigand, J.; Leito, I.; Girod, M.; Antoine, R.; Kruve, A. Think Negative: Finding the best ESI/MS mode for your analyte. *Anal. Chem.*, 2017, DOI: 10.1021/acs.analchem.7b00096.

Teaching work:

Supervision

1. Kerli Martin, Building binding scales of simple carboxylate anions by synthetic receptors, Master's Degree, 2014.
2. Juuli Nõges, Differentiation of similar receptor-anion binding affinities using an NMR based method, Master's Degree, 2016.
3. Indrek Saar, Influence of water on the binding ability of anion-sensitive molecular receptors, Bachelor's Degree, 2017.

ELULOOKIRJELDUS

Nimi: Kristjan Haav
Sünniaeg: 20.02.1989
Kodakondsus: Eesti
Kontakt: Keemia instituut, loodus- ja tehnoloogiateaduskond,
Tartu Ülikool
Ravila 14a, 50411 Tartu, Eesti
E-post: kristjanhaav@gmail.com

Haridus:

2005–2008	Tartu Mart Reiniku Gümnaasium
2008–2011	Tartu Ülikool, Loodus- ja tehnoloogiateaduskond, bakalaureuseõpe: keemia
2011–2013	Tartu Ülikool, Loodus- ja tehnoloogiateaduskond, magistriõpe: rakenduslik mõõteteadus (*cum laude*)
2013–	Tartu Ülikool, keemia eriala doktorant

Töökogemus: 2012-tänaseni Tartu Ülikool; Keemik

Teaduspublikatsioonid:

1. Haav, K.; Saame, J.; Kütt, A.; Leito, I. Basicity of Phosphanes and Diphosphanes in Acetonitrile. *Eur. J. Org. Chem.*, **2012**, *11*, 2167–2172.
2. Haav, K.; Kadam, S. A.; Toom, L.; Gale, P. A.; Busschaert, N.; Wenzel, M.; Hiscock, J. R.; Kirby, I. L.; Haljasorg, T.; Lõkov, M.; Leito I. Accurate Method To Quantify Binding in Supramolecular Chemistry. *J. Org. Chem.*, **2013**, *78*, 7796–7808.
3. Kadam, S. A.; Haav, K.; Toom, L.; Haljasorg, T.; Leito, I. NMR Method for Simultaneous Host–Guest Binding Constant Measurement. *J. Org. Chem.*, **2014**, *79*, 2501–2513.
4. Kadam, S. A.; Martin, K.; Haav, K.; Toom, L.; Mayeux, C.; Pung, A.; Gale, P. A.; Hiscock, J. R.; Brooks, S. J.; Kirby, I. L.; Busschaert, N.; Leito, I. Towards the Discrimination of Carboxylates by Hydrogen-Bond Donor Anion Receptors. *Chem. Eur. J.*, **2015**, *21*, 5145–5160.
5. Tshepelevitsh, S.; Trummal, A.; Haav, K.; Martin, K.; Leito, I. Hydrogen-Bond Donicity in DMSO and Gas Phase and Its Dependence on Brønsted Acidity. *J. Phys. Chem. A*, **2017**, *121*, 357–369.
6. Kadam, S. A.; Haav, K.; Toom, L.; Pung, A.; Mayeux, C.; Leito, I. Multidentate anion receptors for binding glyphosate dianion: structure and affinity. *Eur. J. Org. Chem.*, **2017**, 1396–1406.
7. Liigand, P.; Kaupmees, K.; Haav, K.; Liigand, J.; Leito, I.; Girod, M.; Antoine, R.; Kruve, A. Think Negative: Finding the best ESI/MS mode for your analyte. *Anal. Chem.*, 2017, DOI: 10.1021/acs.analchem.7b00096.

Õppetöö:

Juhendamine

1. Kerli Martin, Sünteetiliste retseptorite seondumisskaalade koostamine lihtsamatele karboksülaatioonidele, magistrikraad, kaitstud 2014.
2. Juuli Nõges, Lähedaste retseptor-anioon seondumisafiinsuste eristamine TMR meetodil, magistrikraad, kaitstud 2016.
3. Indrek Saar, Keskkonna veesisalduse mõju anioonitundlike retseptorite seondumisvõimele, bakalaureusekraad, kaitstud 2017.

DISSERTATIONES CHIMICAE UNIVERSITATIS TARTUENSIS

1. **Toomas Tamm.** Quantum-chemical simulation of solvent effects. Tartu, 1993, 110 p.
2. **Peeter Burk.** Theoretical study of gas-phase acid-base equilibria. Tartu, 1994, 96 p.
3. **Victor Lobanov.** Quantitative structure-property relationships in large descriptor spaces. Tartu, 1995, 135 p.
4. **Vahur Mäemets.** The ^{17}O and ^{1}H nuclear magnetic resonance study of H_2O in individual solvents and its charged clusters in aqueous solutions of electrolytes. Tartu, 1997, 140 p.
5. **Andrus Metsala.** Microcanonical rate constant in nonequilibrium distribution of vibrational energy and in restricted intramolecular vibrational energy redistribution on the basis of slater's theory of unimolecular reactions. Tartu, 1997, 150 p.
6. **Uko Maran.** Quantum-mechanical study of potential energy surfaces in different environments. Tartu, 1997, 137 p.
7. **Alar Jänes.** Adsorption of organic compounds on antimony, bismuth and cadmium electrodes. Tartu, 1998, 219 p.
8. **Kaido Tammeveski.** Oxygen electroreduction on thin platinum films and the electrochemical detection of superoxide anion. Tartu, 1998, 139 p.
9. **Ivo Leito.** Studies of Brønsted acid-base equilibria in water and non-aqueous media. Tartu, 1998, 101 p.
10. **Jaan Leis.** Conformational dynamics and equilibria in amides. Tartu, 1998, 131 p.
11. **Toonika Rinken.** The modelling of amperometric biosensors based on oxidoreductases. Tartu, 2000, 108 p.
12. **Dmitri Panov.** Partially solvated Grignard reagents. Tartu, 2000, 64 p.
13. **Kaja Orupõld.** Treatment and analysis of phenolic wastewater with microorganisms. Tartu, 2000, 123 p.
14. **Jüri Ivask.** Ion Chromatographic determination of major anions and cations in polar ice core. Tartu, 2000, 85 p.
15. **Lauri Vares.** Stereoselective Synthesis of Tetrahydrofuran and Tetrahydropyran Derivatives by Use of Asymmetric Horner-Wadsworth-Emmons and Ring Closure Reactions. Tartu, 2000, 184 p.
16. **Martin Lepiku.** Kinetic aspects of dopamine D_2 receptor interactions with specific ligands. Tartu, 2000, 81 p.
17. **Katrin Sak.** Some aspects of ligand specificity of P2Y receptors. Tartu, 2000, 106 p.
18. **Vello Pällin.** The role of solvation in the formation of iotsitch complexes. Tartu, 2001, 95 p.
19. **Katrin Kollist.** Interactions between polycyclic aromatic compounds and humic substances. Tartu, 2001, 93 p.

20. **Ivar Koppel.** Quantum chemical study of acidity of strong and superstrong Brønsted acids. Tartu, 2001, 104 p.
21. **Viljar Pihl.** The study of the substituent and solvent effects on the acidity of OH and CH acids. Tartu, 2001, 132 p.
22. **Natalia Palm.** Specification of the minimum, sufficient and significant set of descriptors for general description of solvent effects. Tartu, 2001, 134 p.
23. **Sulev Sild.** QSPR/QSAR approaches for complex molecular systems. Tartu, 2001, 134 p.
24. **Ruslan Petrukhin.** Industrial applications of the quantitative structure-property relationships. Tartu, 2001, 162 p.
25. **Boris V. Rogovoy.** Synthesis of (benzotriazolyl)carboximidamides and their application in relations with *N*- and *S*-nucleophyles. Tartu, 2002, 84 p.
26. **Koit Herodes.** Solvent effects on UV-vis absorption spectra of some solvatochromic substances in binary solvent mixtures: the preferential solvation model. Tartu, 2002, 102 p.
27. **Anti Perkson.** Synthesis and characterisation of nanostructured carbon. Tartu, 2002, 152 p.
28. **Ivari Kaljurand.** Self-consistent acidity scales of neutral and cationic Brønsted acids in acetonitrile and tetrahydrofuran. Tartu, 2003, 108 p.
29. **Karmen Lust.** Adsorption of anions on bismuth single crystal electrodes. Tartu, 2003, 128 p.
30. **Mare Piirsalu.** Substituent, temperature and solvent effects on the alkaline hydrolysis of substituted phenyl and alkyl esters of benzoic acid. Tartu, 2003, 156 p.
31. **Meeri Sassian.** Reactions of partially solvated Grignard reagents. Tartu, 2003, 78 p.
32. **Tarmo Tamm.** Quantum chemical modelling of polypyrrole. Tartu, 2003. 100 p.
33. **Erik Teinemaa.** The environmental fate of the particulate matter and organic pollutants from an oil shale power plant. Tartu, 2003. 102 p.
34. **Jaana Tammiku-Taul.** Quantum chemical study of the properties of Grignard reagents. Tartu, 2003. 120 p.
35. **Andre Lomaka.** Biomedical applications of predictive computational chemistry. Tartu, 2003. 132 p.
36. **Kostyantyn Kirichenko.** Benzotriazole – Mediated Carbon–Carbon Bond Formation. Tartu, 2003. 132 p.
37. **Gunnar Nurk.** Adsorption kinetics of some organic compounds on bismuth single crystal electrodes. Tartu, 2003, 170 p.
38. **Mati Arulepp.** Electrochemical characteristics of porous carbon materials and electrical double layer capacitors. Tartu, 2003, 196 p.
39. **Dan Cornel Fara.** QSPR modeling of complexation and distribution of organic compounds. Tartu, 2004, 126 p.
40. **Riina Mahlapuu.** Signalling of galanin and amyloid precursor protein through adenylate cyclase. Tartu, 2004, 124 p.

41. **Mihkel Kerikmäe.** Some luminescent materials for dosimetric applications and physical research. Tartu, 2004, 143 p.
42. **Jaanus Kruusma.** Determination of some important trace metal ions in human blood. Tartu, 2004, 115 p.
43. **Urmas Johanson.** Investigations of the electrochemical properties of polypyrrole modified electrodes. Tartu, 2004, 91 p.
44. **Kaido Sillar.** Computational study of the acid sites in zeolite ZSM-5. Tartu, 2004, 80 p.
45. **Aldo Oras.** Kinetic aspects of dATPαS interaction with $P2Y_1$ receptor. Tartu, 2004, 75 p.
46. **Erik Mölder.** Measurement of the oxygen mass transfer through the air-water interface. Tartu, 2005, 73 p.
47. **Thomas Thomberg.** The kinetics of electroreduction of peroxodisulfate anion on cadmium (0001) single crystal electrode. Tartu, 2005, 95 p.
48. **Olavi Loog.** Aspects of condensations of carbonyl compounds and their imine analogues. Tartu, 2005, 83 p.
49. **Siim Salmar.** Effect of ultrasound on ester hydrolysis in aqueous ethanol. Tartu, 2006, 73 p.
50. **Ain Uustare.** Modulation of signal transduction of heptahelical receptors by other receptors and G proteins. Tartu, 2006, 121 p.
51. **Sergei Yurchenko.** Determination of some carcinogenic contaminants in food. Tartu, 2006, 143 p.
52. **Kaido Tämm.** QSPR modeling of some properties of organic compounds. Tartu, 2006, 67 p.
53. **Olga Tšubrik.** New methods in the synthesis of multisubstituted hydrazines. Tartu. 2006, 183 p.
54. **Lilli Sooväli.** Spectrophotometric measurements and their uncertainty in chemical analysis and dissociation constant measurements. Tartu, 2006, 125 p.
55. **Eve Koort.** Uncertainty estimation of potentiometrically measured ph and pK_a values. Tartu, 2006, 139 p.
56. **Sergei Kopanchuk.** Regulation of ligand binding to melanocortin receptor subtypes. Tartu, 2006, 119 p.
57. **Silvar Kallip.** Surface structure of some bismuth and antimony single crystal electrodes. Tartu, 2006, 107 p.
58. **Kristjan Saal.** Surface silanization and its application in biomolecule coupling. Tartu, 2006, 77 p.
59. **Tanel Tätte.** High viscosity $Sn(OBu)_4$ oligomeric concentrates and their applications in technology. Tartu, 2006, 91 p.
60. **Dimitar Atanasov Dobchev**. Robust QSAR methods for the prediction of properties from molecular structure. Tartu, 2006, 118 p.
61. **Hannes Hagu**. Impact of ultrasound on hydrophobic interactions in solutions. Tartu, 2007, 81 p.

62. **Rutha Jäger.** Electroreduction of peroxodisulfate anion on bismuth electrodes. Tartu, 2007, 142 p.
63. **Kaido Viht.** Immobilizable bisubstrate-analogue inhibitors of basophilic protein kinases: development and application in biosensors. Tartu, 2007, 88 p.
64. **Eva-Ingrid Rõõm.** Acid-base equilibria in nonpolar media. Tartu, 2007, 156 p.
65. **Sven Tamp.** DFT study of the cesium cation containing complexes relevant to the cesium cation binding by the humic acids. Tartu, 2007, 102 p.
66. **Jaak Nerut.** Electroreduction of hexacyanoferrate(III) anion on Cadmium (0001) single crystal electrode. Tartu, 2007, 180 p.
67. **Lauri Jalukse.** Measurement uncertainty estimation in amperometric dissolved oxygen concentration measurement. Tartu, 2007, 112 p.
68. **Aime Lust.** Charge state of dopants and ordered clusters formation in CaF_2:Mn and CaF_2:Eu luminophors. Tartu, 2007, 100 p.
69. **Iiris Kahn**. Quantitative Structure-Activity Relationships of environmentally relevant properties. Tartu, 2007, 98 p.
70. **Mari Reinik.** Nitrates, nitrites, N-nitrosamines and polycyclic aromatic hydrocarbons in food: analytical methods, occurrence and dietary intake. Tartu, 2007, 172 p.
71. **Heili Kasuk.** Thermodynamic parameters and adsorption kinetics of organic compounds forming the compact adsorption layer at Bi single crystal electrodes. Tartu, 2007, 212 p.
72. **Erki Enkvist.** Synthesis of adenosine-peptide conjugates for biological applications. Tartu, 2007, 114 p.
73. **Svetoslav Hristov Slavov**. Biomedical applications of the QSAR approach. Tartu, 2007, 146 p.
74. **Eneli Härk.** Electroreduction of complex cations on electrochemically polished Bi(*hkl*) single crystal electrodes. Tartu, 2008, 158 p.
75. **Priit Möller.** Electrochemical characteristics of some cathodes for medium temperature solid oxide fuel cells, synthesized by solid state reaction technique. Tartu, 2008, 90 p.
76. **Signe Viggor.** Impact of biochemical parameters of genetically different pseudomonads at the degradation of phenolic compounds. Tartu, 2008, 122 p.
77. **Ave Sarapuu.** Electrochemical reduction of oxygen on quinone-modified carbon electrodes and on thin films of platinum and gold. Tartu, 2008, 134 p.
78. **Agnes Kütt.** Studies of acid-base equilibria in non-aqueous media. Tartu, 2008, 198 p.
79. **Rouvim Kadis.** Evaluation of measurement uncertainty in analytical chemistry: related concepts and some points of misinterpretation. Tartu, 2008, 118 p.
80. **Valter Reedo.** Elaboration of IVB group metal oxide structures and their possible applications. Tartu, 2008, 98 p.

81. **Aleksei Kuznetsov.** Allosteric effects in reactions catalyzed by the cAMP-dependent protein kinase catalytic subunit. Tartu, 2009, 133 p.
82. **Aleksei Bredihhin.** Use of mono- and polyanions in the synthesis of multisubstituted hydrazine derivatives. Tartu, 2009, 105 p.
83. **Anu Ploom.** Quantitative structure-reactivity analysis in organosilicon chemistry. Tartu, 2009, 99 p.
84. **Argo Vonk.** Determination of adenosine A_{2A}- and dopamine D_1 receptor-specific modulation of adenylate cyclase activity in rat striatum. Tartu, 2009, 129 p.
85. **Indrek Kivi.** Synthesis and electrochemical characterization of porous cathode materials for intermediate temperature solid oxide fuel cells. Tartu, 2009, 177 p.
86. **Jaanus Eskusson.** Synthesis and characterisation of diamond-like carbon thin films prepared by pulsed laser deposition method. Tartu, 2009, 117 p.
87. **Marko Lätt.** Carbide derived microporous carbon and electrical double layer capacitors. Tartu, 2009, 107 p.
88. **Vladimir Stepanov.** Slow conformational changes in dopamine transporter interaction with its ligands. Tartu, 2009, 103 p.
89. **Aleksander Trummal.** Computational Study of Structural and Solvent Effects on Acidities of Some Brønsted Acids. Tartu, 2009, 103 p.
90. **Eerold Vellemäe.** Applications of mischmetal in organic synthesis. Tartu, 2009, 93 p.
91. **Sven Parkel.** Ligand binding to 5-HT_{1A} receptors and its regulation by Mg^{2+} and Mn^{2+}. Tartu, 2010, 99 p.
92. **Signe Vahur.** Expanding the possibilities of ATR-FT-IR spectroscopy in determination of inorganic pigments. Tartu, 2010, 184 p.
93. **Tavo Romann**. Preparation and surface modification of bismuth thin film, porous, and microelectrodes. Tartu, 2010, 155 p.
94. **Nadežda Aleksejeva.** Electrocatalytic reduction of oxygen on carbon nanotube-based nanocomposite materials. Tartu, 2010, 147 p.
95. **Marko Kullapere.** Electrochemical properties of glassy carbon, nickel and gold electrodes modified with aryl groups. Tartu, 2010, 233 p.
96. **Liis Siinor.** Adsorption kinetics of ions at Bi single crystal planes from aqueous electrolyte solutions and room-temperature ionic liquids. Tartu, 2010, 101 p.
97. **Angela Vaasa.** Development of fluorescence-based kinetic and binding assays for characterization of protein kinases and their inhibitors. Tartu 2010, 101 p.
98. **Indrek Tulp.** Multivariate analysis of chemical and biological properties. Tartu 2010, 105 p.
99. **Aare Selberg.** Evaluation of environmental quality in Northern Estonia by the analysis of leachate. Tartu 2010, 117 p.
100. **Darja Lavõgina.** Development of protein kinase inhibitors based on adenosine analogue-oligoarginine conjugates. Tartu 2010, 248 p.

101. **Laura Herm.** Biochemistry of dopamine D_2 receptors and its association with motivated behaviour. Tartu 2010, 156 p.
102. **Terje Raudsepp.** Influence of dopant anions on the electrochemical properties of polypyrrole films. Tartu 2010, 112 p.
103. **Margus Marandi.** Electroformation of Polypyrrole Films: *In-situ* AFM and STM Study. Tartu 2011, 116 p.
104. **Kairi Kivirand.** Diamine oxidase-based biosensors: construction and working principles. Tartu, 2011, 140 p.
105. **Anneli Kruve.** Matrix effects in liquid-chromatography electrospray mass-spectrometry. Tartu, 2011, 156 p.
106. **Gary Urb.** Assessment of environmental impact of oil shale fly ash from PF and CFB combustion. Tartu, 2011, 108 p.
107. **Nikita Oskolkov.** A novel strategy for peptide-mediated cellular delivery and induction of endosomal escape. Tartu, 2011, 106 p.
108. **Dana Martin.** The QSPR/QSAR approach for the prediction of properties of fullerene derivatives. Tartu, 2011, 98 p.
109. **Säde Viirlaid.** Novel glutathione analogues and their antioxidant activity. Tartu, 2011, 106 p.
110. **Ülis Sõukand.** Simultaneous adsorption of Cd^{2+}, Ni^{2+}, and Pb^{2+} on peat. Tartu, 2011, 124 p.
111. **Lauri Lipping.** The acidity of strong and superstrong Brønsted acids, an outreach for the "limits of growth": a quantum chemical study. Tartu, 2011, 124 p.
112. **Heisi Kurig.** Electrical double-layer capacitors based on ionic liquids as electrolytes. Tartu, 2011, 146 p.
113. **Marje Kasari.** Bisubstrate luminescent probes, optical sensors and affinity adsorbents for measurement of active protein kinases in biological samples. Tartu, 2012, 126 p.
114. **Kalev Takkis.** Virtual screening of chemical databases for bioactive molecules. Tartu, 2012, 122 p.
115. **Ksenija Kisseljova**. Synthesis of aza-β^3-amino acid containing peptides and kinetic study of their phosphorylation by protein kinase A. Tartu, 2012, 104 p.
116. **Riin Rebane.** Advanced method development strategy for derivatization LC/ESI/MS. Tartu, 2012, 184 p.
117. **Vladislav Ivaništšev.** Double layer structure and adsorption kinetics of ions at metal electrodes in room temperature ionic liquids. Tartu, 2012, 128 p.
118. **Irja Helm.** High accuracy gravimetric Winkler method for determination of dissolved oxygen. Tartu, 2012, 139 p.
119. **Karin Kipper.** Fluoroalcohols as Components of LC-ESI-MS Eluents: Usage and Applications. Tartu, 2012, 164 p.
120. **Arno Ratas.** Energy storage and transfer in dosimetric luminescent materials. Tartu, 2012, 163 p.

121. **Reet Reinart-Okugbeni**. Assay systems for characterisation of subtype-selective binding and functional activity of ligands on dopamine receptors. Tartu, 2012, 159 p.
122. **Lauri Sikk.** Computational study of the Sonogashira cross-coupling reaction. Tartu, 2012, 81 p.
123. **Karita Raudkivi.** Neurochemical studies on inter-individual differences in affect-related behaviour of the laboratory rat. Tartu, 2012, 161 p.
124. **Indrek Saar.** Design of GalR2 subtype specific ligands: their role in depression-like behavior and feeding regulation. Tartu, 2013, 126 p.
125. **Ann Laheäär.** Electrochemical characterization of alkali metal salt based non-aqueous electrolytes for supercapacitors. Tartu, 2013, 127 p.
126. **Kerli Tõnurist.** Influence of electrospun separator materials properties on electrochemical performance of electrical double-layer capacitors. Tartu, 2013, 147 p.
127. **Kaija Põhako-Esko.** Novel organic and inorganic ionogels: preparation and characterization. Tartu, 2013, 124 p.
128. **Ivar Kruusenberg.** Electroreduction of oxygen on carbon nanomaterial-based catalysts. Tartu, 2013, 191 p.
129. **Sander Piiskop.** Kinetic effects of ultrasound in aqueous acetonitrile solutions. Tartu, 2013, 95 p.
130. **Ilona Faustova**. Regulatory role of L-type pyruvate kinase N-terminal domain. Tartu, 2013, 109 p.
131. **Kadi Tamm.** Synthesis and characterization of the micro-mesoporous anode materials and testing of the medium temperature solid oxide fuel cell single cells. Tartu, 2013, 138 p.
132. **Iva Bozhidarova Stoyanova-Slavova.** Validation of QSAR/QSPR for regulatory purposes. Tartu, 2013, 109 p.
133. **Vitali Grozovski**. Adsorption of organic molecules at single crystal electrodes studied by *in situ* STM method. Tartu, 2014, 146 p.
134. **Santa Veikšina**. Development of assay systems for characterisation of ligand binding properties to melanocortin 4 receptors. Tartu, 2014, 151 p.
135. **Jüri Liiv.** PVDF (polyvinylidene difluoride) as material for active element of twisting-ball displays. Tartu, 2014, 111 p.
136. **Kersti Vaarmets.** Electrochemical and physical characterization of pristine and activated molybdenum carbide-derived carbon electrodes for the oxygen electroreduction reaction. Tartu, 2014, 131 p.
137. **Lauri Tõntson**. Regulation of G-protein subtypes by receptors, guanine nucleotides and Mn^{2+}. Tartu, 2014, 105 p.
138. **Aiko Adamson.** Properties of amine-boranes and phosphorus analogues in the gas phase. Tartu, 2014, 78 p.
139. **Elo Kibena**. Electrochemical grafting of glassy carbon, gold, highly oriented pyrolytic graphite and chemical vapour deposition-grown graphene electrodes by diazonium reduction method. Tartu, 2014, 184 p.

140. **Teemu Näykki.** Novel Tools for Water Quality Monitoring – From Field to Laboratory. Tartu, 2014, 202 p.
141. **Karl Kaupmees.** Acidity and basicity in non-aqueous media: importance of solvent properties and purity. Tartu, 2014, 128 p.
142. **Oleg Lebedev**. Hydrazine polyanions: different strategies in the synthesis of heterocycles. Tartu, 2015, 118 p.
143. **Geven Piir.** Environmental risk assessment of chemicals using QSAR methods. Tartu, 2015, 123 p.
144. **Olga Mazina.** Development and application of the biosensor assay for measurements of cyclic adenosine monophosphate in studies of G protein-coupled receptor signalinga. Tartu, 2015, 116 p.
145. **Sandip Ashokrao Kadam.** Anion receptors: synthesis and accurate binding measurements. Tartu, 2015, 116 p.
146. **Indrek Tallo.** Synthesis and characterization of new micro-mesoporous carbide derived carbon materials for high energy and power density electrical double layer capacitors. Tartu, 2015, 148 p.
147. **Heiki Erikson.** Electrochemical reduction of oxygen on nanostructured palladium and gold catalysts. Tartu, 2015, 204 p.
148. **Erik Anderson.** *In situ* Scanning Tunnelling Microscopy studies of the interfacial structure between Bi(111) electrode and a room temperature ionic liquid. Tartu, 2015, 118 p.
149. **Girinath G. Pillai.** Computational Modelling of Diverse Chemical, Bio-chemical and Biomedical Properties. Tartu, 2015, 140 p.
150. **Piret Pikma.** Interfacial structure and adsorption of organic compounds at Cd(0001) and Sb(111) electrodes from ionic liquid and aqueous electrolytes: an *in situ* STM study. Tartu, 2015, 126 p.
151. **Ganesh babu Manoharan.** Combining chemical and genetic approaches for photoluminescence assays of protein kinases. Tartu, 2016, 126 p.
152. **Carolin Siimenson**. Electrochemical characterization of halide ion adsorption from liquid mixtures at Bi(111) and pyrolytic graphite electrode surface. Tartu, 2016, 110 p.
153. **Asko Laaniste.** Comparison and optimisation of novel mass spectrometry ionisation sources. Tartu, 2016, 156 p.
154. **Hanno Evard.** Estimating limit of detection for mass spectrometric analysis methods. Tartu, 2016, 224 p.
155. **Kadri Ligi.** Characterization and application of protein kinase-responsive organic probes with triplet-singlet energy transfer. Tartu, 2016, 122 p.
156. **Margarita Kagan.** Biosensing penicillins' residues in milk flows. Tartu, 2016, 130 p.
157. **Marie Kriisa.** Development of protein kinase-responsive photo-luminescent probes and cellular regulators of protein phosphorylation. Tartu, 2016, 106 p.
158. **Mihkel Vestli.** Ultrasonic spray pyrolysis deposited electrolyte layers for intermediate temperature solid oxide fuel cells. Tartu, 2016, 156 p.

159. **Silver Sepp.** Influence of porosity of the carbide-derived carbon on the properties of the composite electrocatalysts and characteristics of polymer electrolyte fuel cells. Tartu, 2016, 137 p.